Dalton Transactions

PAPER

View Article Online
View Journal | View Issue

Cite this: *Dalton Trans.*, 2025, **54**, 15306

Rhodium(I) complexes with proton-responsive anionic tethered N-heterocyclic carbene ligands: synthesis and application in alkyne dimerization

Mert Olgun Karataş, *[a,b] Diego R. Hinojosa, [a] Vincenzo Passarelli, [a]
Luis A. Oro, [a] Jesús J. Pérez-Torrente [a] and Ricardo Castarlenas *[a]

Received 26th June 2025,
Accepted 18th September 2025

DOI: 10.1039/d5dt01516b

rsc.li/dalton

A series of rhodium(I) complexes of formula Rh{κ^2*C*,*X*-(I$^{\mathrm{Dipp}}$R)}(cod) and Rh{κ^2*C*,*X*-(I$^{\mathrm{Dipp}}$R)}(CO)$_2$ {I$^{\mathrm{Dipp}}$R = 1-(R)-3-(2,6-diisopropylphenyl)-imidazolin-2-carbene; X = N, O; R = (6-yl-2-pyridone), (CH$_2$CH$_2$NC(=O)Ph), (CH$_2$CH$_2$COO); (cod = 1,5-cyclooctadiene)} containing anionic-tethered NHC-functionalized ligands, including pyridonato, amidato or carboxylato groups at the *N*-wingtip, has been prepared and their application to alkyne homocoupling has been investigated. The chelate coordination of the NHC-functionalized ligand generates 5, 6 and 7-membered metallacycles for pyridonato, amidato and carboxylato substituents, respectively. Preparation of the mixed bis-NHC derivative Rh{κ^2*C*,*O*-(I$^{\mathrm{Dipp}}$Carbx)}(CO)(IPr) {IPr = 1,3-bis-(2,6-diisopropylphenyl)-imidazolin-2-carbene} is possible due to lability of one of the CO ligands in the bis-CO precursor. Reversible protonation is observed for pyridonato and carboxylato moieties but not for amidato counterpart. Alkyne dimerization catalytic activity is reported for *N*-based anionic groups whereas carboxylato counterparts are inefficient. A proton transfer mechanism is invoked for the *gem*-selectivity observed for cod-based catalysts whereas alkyne insertion is the regioselectivity-determining step for CO-containing analogues.

Introduction

N-Heterocyclic Carbenes (NHCs)[1] are fascinating molecules with widespread applications ranging from biomedicine[2] to materials science,[3] but are particularly prominent in catalysis.[4] Their unique structural framework allows for fairly unlimited design possibilities, driving the development of a myriad of mild-condition synthetic methods.[5] Notably, the incorporation of a non-spectator functional group on the *N*-wingtip has enabled their participation in very efficient Metal–Ligand Cooperative (MLC) transformations.[6] In this context, functional groups based on O,[7] N,[8] P,[9] S,[10] and Si[11] heteroatoms, as well as carbon-based substituents,[12] have been reported. Moreover, these types of bidentate or multidentate ligands could also play a crucial role in catalysis by stabilizing low-coordinated active species.[13] In particular, NHCs decorated with deprotonatable moieties, such as pyridone,[14] amide[15] or carboxylic acids,[16] have been successfully used to prepare anionic tethered NHC–metal catalysts (Chart 1a). The benefits of these pendant scaffolds are not limited to acting as internal bases that facilitate proton transfer processes, but also extend to modulating catalytic activity and selectivity through interactions with the metal center or substrates. Indeed, they prevent catalyst decomposition in acidic environments through imidazolium salt formation,[17] where the pendant basic group act as a proton sponge that inhibits metal–NHC bond cleavage.[18]

Alkyne dimerization is a straightforward and atom-economical route to 1,3-enynes, which are key structural motifs in a variety of biologically active molecules or functional materials.[19] However, achieving high chemo-, regio- and stereoselectivity is a challenging task due to a multifaceted mechanistic scenario,[20] which also includes competing pathways leading to cyclotrimers,[21] polymers,[22] butatrienes[23] or other complex cyclic structures such as fulvenes,[24] pentalenes,[25] azulenes,[26] or bicyclooctatrienes.[27] While a few selective catalysts for *E*-,[28] *Z*-[29] or *gem*-enynes[12b,30] have been developed, further research is warranted not only to improve catalyst efficiency but also to gain deeper mechanistic insights that could be valuable for other C–H activation and C–C coupling transformations. In general, alkyne migratory insertion into metal–hydride or metal–alkynyl bonds is the rate- and regioselectivity-determining step.[31] However, proton transfer processes from the terminal position of one alkyne to another have been demonstrated to be highly efficient alternative pathways.[32] In this context, our group recently reported highly

---

[a] Instituto de Síntesis Química y Catálisis Homogénea (ISQCH)-Departamento de Química Inorgánica, CSIC-Universidad de Zaragoza, C/Pedro Cerbuna 12, CP. 50009 Zaragoza, Spain. E-mail: mkaratas@unizar.es, rcastar@unizar.es
[b] Department of Chemistry, Faculty of Sciences, Inönü University, 44280 Malatya, Turkey

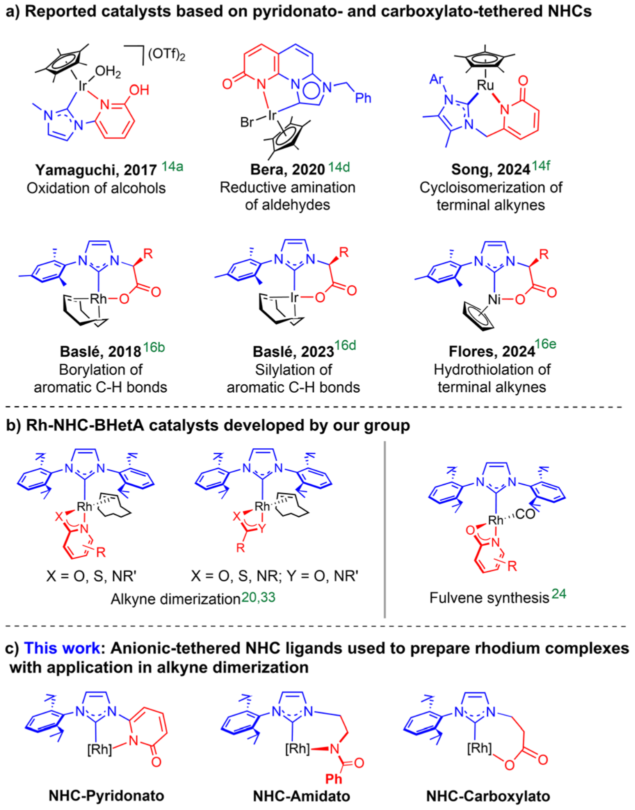

Chart 1 (a) Selected examples of catalysts with pyridonato- and carboxylato-tethered NHC ligands. (b) Rh–NHC–BHetA catalysts for alkyne functionalization. (c) Complexes prepared in this work.

active Rh–NHC catalysts for the specific head-to-tail dimerization of alkynes to form 1,3-*gem*-enynes *via* a Ligand Assisted Proton Shuttle (LAPS) mechanism.[20,33] We found that Bis-Heteroatomic Acidato ligands (BHetA), such as carboxylato, amidato, amidinato, and especially pyridonato, can act as efficient proton transfer agents, enhancing activity and selectivity (Chart 1b). Based on these findings, we envisage the potential of rhodium complexes bearing nitrogen- and oxygen-tethered NHC ligands as effective proton carriers for catalytic applications. Herein, we report on the synthesis of Rh(I) complexes with pyridonato-, amidato-, and carboxylato tethered-NHCs and their performance as alkyne dimerization catalysts.

Results and discussion

Synthesis and characterization of NHC-pyridonato Rh(I) complexes

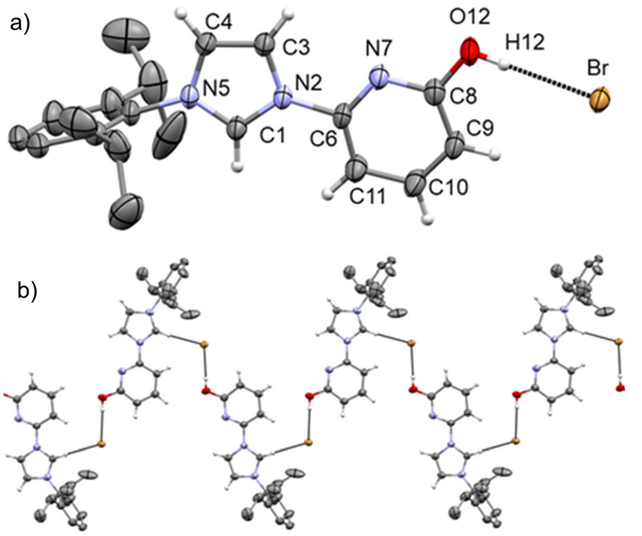

Fig. 1 (a) ORTEP views of the crystal structure of **1**. For clarity, most hydrogen atoms are omitted. Thermal ellipsoids are at 50% probability. (b) Intermolecular $I^{Dipp}OpyH_2\cdots Br$ contacts along the b axis. Selected bond lengths (Å) and angles (°) are: C1–N2 1.338(4), C1–N5 1.329(4), C3–N2 1.382(4), C3–C4 1.352(4), C4–N5 1.383(4), C6–N2 1.445(3), C6–N7 1.325(4), C6–C11 1.363(4), C8–N7 1.331(4), C8–C9 1.400(5), C8–O12 1.341(4), C9–C10 1.370(5), C10–C11 1.398(4), N7–C6–N2–C1–177.23(27), O12–H12···Br: O12–H12 0.840(2), H12–Br 2.372(1), O12–Br, 3.211(2), O12–H12–Br 176.66(16), C1–H1···Br#: C1–H1 0.950(3), H1–Br# 2.584(1), C1–Br# 3.532(3), C1–H1–Br# 175.82(18), # equivalent position: −*x* + 1/2 + 1, +*y* + 1/2, −*z* + 1/2.

The 1-(6-hydroxypyridin-2-yl)-3-(2,6-diisopropylphenyl)-imidazol-3-ium bromide salt [$I^{Dipp}OpyH_2$]Br (**1**) was prepared according to previously described procedures.[34] In view of the tautomeric equilibrium[35] of the heterocyclic tether between pyridone[34a] or hydroxypyridine[34b] isomer, the X-ray diffraction analysis of **1** was carried out (Fig. 1). As a matter of fact, the crystal structure of **1** revealed that the salt adopts the hydroxypyridine tautomeric form (Fig. 1a). In agreement with the presence of the OH group, the C8–O12 bond length [1.341(4) Å] is similar to that reported for C^{arom}–O single bonds [1.362 Å, av.].[36] The asymmetric unit of the crystal structure of **1** contains the ion pair $I^{Dipp}OpyH_2$/bromide. Within the $I^{Dipp}OpyH_2$ cation, the aromatic ring of the 2,6-$^iPr_2C_6H_3$ group lies almost perpendicular to the NHC core, whereas the hydroxypyridinyl fragment and the NHC core are nearly coplanar [O12–H12–Br 176.66(16)°]. Notably, O12–H12···Br and the C1–H1···Br intermolecular contacts are observed, thus rendering infinite chains growing along the b axis (Fig. 1b).

Metalation of the ligand was achieved by treatment of **1** with [Rh(μ-Cl)(cod)]$_2$ (cod = 1,5-cyclooctadiene) in the presence of 3 equivalents of ^{t}BuOK in THF for 30 min. The mononuclear chelate complex Rh{κ^2*C*,*N*-(I^{Dipp}Opy)}(cod) (**2**) was obtained as a result of the deprotonation of both the imidazolium and hydroxypyridine moieties (Scheme 1). In contrast to **1**, the pyridonato tautomeric form of the tether was observed

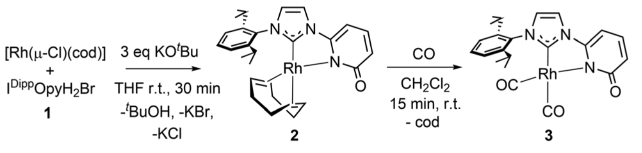

Scheme 1 Preparation of pyridonato-functionalized NHC rhodium derivatives **2** and **3**.

in **2**. The use of an excess of base was deemed to be essential to incorporate the NHC-functionalized ligand into the metal center. In fact, several attempts to prepare the putative Rh(I) derivative RhX{κ*C*-(I^{Dipp}OpyH)}(cod) by selective deprotonation of the imidazolium fragment were unsuccessful. Moreover, the use of the monoolefin complex $[Rh(\mu\text{-}Cl)(\eta^2\text{-}coe)_2]_2$ (coe = cyclooctene) as a synthetic precursor resulted in a mixture of unidentified products. Bubbling carbon monoxide through a CH_2Cl_2 solution of **2** afforded the bis-carbonyl compound Rh{κ^2*C*,*N*-(I^{Dipp}Opy)}$(CO)_2$ **3**, which was isolated as a yellow solid in 78% yield.

The solid-state structure of **2** was determined by X-ray diffraction analysis on single crystals obtained by slow diffusion of *n*-hexane into a concentrated $CDCl_3$ solution of **2** (Fig. 2). The crystal structure of **2** shows a square planar coordination polyhedron at the metal centre given by the bidentate cod and I^{Dipp}Opy ligands. As consequence of the short bite angles C1–Rh–N7 [78.37(12)°] both the NHC and the pyridine moieties of the I^{Dipp}Opy ligand strongly deviate from the ideal arrangement with respect to the Rh–C1 and Rh–N7 bonds (NHC: pitch ϑ 1.2° yaw ψ 14.3°; py: pitch ϑ 7.0°; yaw ψ 7.0°).[37] Notably, when comparing the C8–O12 bond lengths in **1** [1.341(4) Å] and **2** [1.247(4) Å], the short C8–O12 bond length of **2** is indicative of the fact that the I^{Dipp}Opy moiety switches from a hydroxypyridine motif in **1** to a pyridonato scaffold in **2** upon deprotonation and coordination to rhodium.

The NMR spectra of **2** are in agreement with the structure observed in the solid state. The appearance of only one septuplet at δ 2.72 ppm for the two CH-isopropyl protons along with two multiplets at δ 6.18 and 3.50 ppm for the CH moieties of the cod ligand in the ^1H NMR spectrum of **2**, indicates an in-plane disposition of the NHC moiety relative to the metal coordination plane. This molecular topology defines a plane of symmetry that includes the imidazole and pyridone rings and bisects both the Dipp and cod groups. The assignment of the two doublets at δ 7.40 and 6.66 ppm, corresponding to the imidazolinyl protons, is inferred from their NOE correlations with the pyridonato and CH-isopropyl protons, respectively (Fig. 3a). The most characteristic signals in the $^{13}C\{^1H\}$-APT spectrum are the three doublets observed for the carbon atoms coordinated to the rhodium center at δ 174.7 ppm (J_{C-Rh} = 56.6 Hz) for the carbene, 105.0 ppm (J_{C-Rh} = 6.7 Hz) for the *trans*-to-NHC cod, and 70.8 ppm (J_{C-Rh} = 12.4 Hz) for the *cis*-to-NHC cod. Additionally, coordination of the nitrogen atom of the pyridonato tether to form a five-membered metallacycle is confirmed by the long range ^1H–^{15}N HSQC NMR experiment (Fig. 3b). A correlation peak is observed at δ_N 195.8 ppm, which falls within the typical range reported for Rh-κ*N*-pyridonato species, but is approximately 20 ppm more shielded than that of uncoordinated pyridine-2-olato κ*O*-derivatives.[24] Concurrently, the carbene ligand of the bis-carbonyl complex **3** also adopt an in-plane disposition, as evidenced by the observation of only one resonance for the CH-isopropyl protons. Moreover, the $^{13}C\{^1H\}$-APT spectrum of **3**

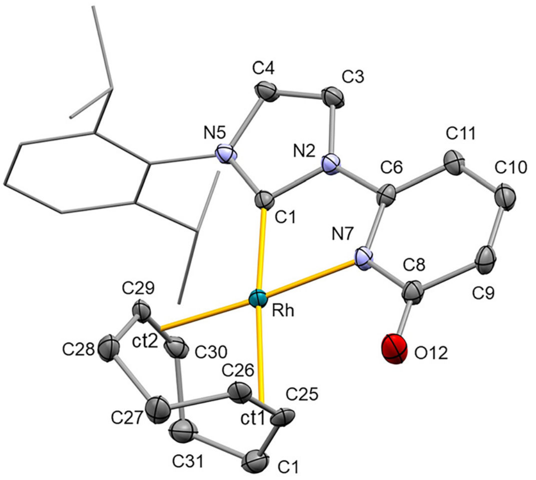

Fig. 2 ORTEP view of the crystal structure of Rh{κ^2*C*,*N*-(I^{Dipp}Opy)}(cod) (**2**). For clarity, hydrogen atoms are omitted and the 2,6-$^iPr_2C_6H_3$ group is shown in a wireframe style. Thermal ellipsoids are at 50% probability. Selected bond lengths (Å) and angles (°) are: C1–Rh 2.015(3), N7–Rh 2.140(3), Rh–ct1 2.121(3), Rh–ct2 1.993(3), C6–N7 1.355(4), C6–C11 1.365(5), C6–N2 1.411(4), C8–N7 1.388(4), C8–O12 1.247(4), C8–C9 1.440(5), C9–C10 1.362(5), C10–C11 1.403(5), C(25)–C(26) 1.374(5), C(29)–C(30) 1.393(5), C1–Rh–N7 78.37(12), ct1–Rh–ct2 86.34(13), N7–C6–N2–C1–3.83(15); ct1, centroid of C25 and C26; ct2, centroid of C29 and C30.

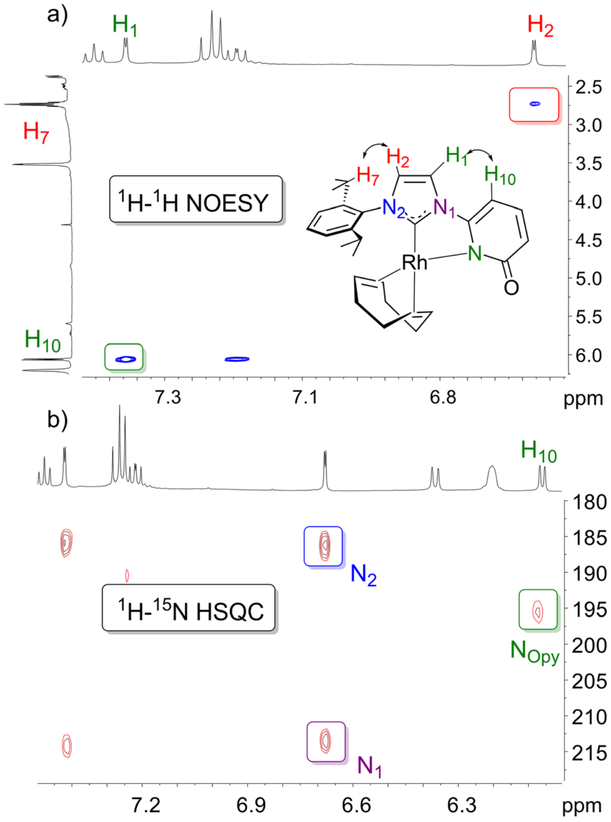

Fig. 3 (a) Selected regions of the 2D-NOESY for **2**. (b) Long range ^1H–^{15}N HSQC NMR spectrum.

confirms the presence of two carbonyl ligands resonating at δ 188.1 ppm (J_{C-Rh} = 57.0 Hz) and 187.3 ppm (J_{C-Rh} = 68.1 Hz).

Synthesis and characterization of NHC-amidato Rh(I) complexes

With the aim of introducing a basic amidato substituent into the NHC framework, the new 1-(2-benzamidoethyl)-3-(2,6-diisopropylphenyl)-imidazol-3-ium chloride salt (**4**) was synthesized *via* *N*-alkylation of 1-(2,6-diisopropylphenyl)-imidazole with *N*-(2-chloroethyl)benzamide in 74% yield (Scheme 2). Treatment of **4** with [Rh(μ-Cl)(cod)]$_2$ and 2 equivalents of ^{t}BuOK in THF at room temperature for 16 h led to the formation of the six-membered metallacycle NHC-amidato complex Rh{κ^2*C*,*N*-(I^{Dipp}Amd)}(cod) (**5**). Exchange of cod by CO in **5** was not as straightforward as might be expected. Bubbling CO through a CH$_2$Cl$_2$ solution of **5** for 15 min afforded the biscarbonyl complex Rh{κ^2*C*,*N*-(I^{Dipp}Amd)}(CO)$_2$ (**6**), together with other unidentified products. In contrast, the transformation proceeds more cleanly upon bubbling CO in THF for only 5 min. It is noteworthy that previous attempts to exchange cod by CO within a related complex were unsuccessful.[15c]

The solid-state structure of **5** was determined by X-ray diffraction analysis on single crystals obtained by slow diffusion of *n*-hexane into a concentrated CH$_2$Cl$_2$ solution of **5** (Fig. 4). The crystal structure of **5** shows a distorted square planar geometry of the metal centre with a κ^2*C*,*N* coordination of the ligand I^{Dipp}Amd, thus confirming the deprotonation of both the imidazolium and the amido moieties. The resulting six-membered metallacycle Rh–C1–N2–C6–C7–N8 adopts a boat conformation with the Rh and C6 atoms in the out-of-plane position. Notably, the atom N8 exhibits a planar geometry [Σ°_{N} = 360.0(3)°] and the C9–O10 [1.263(3) Å] and C9–N8 [C9–N8 1.327(3) Å] bond lengths are similar to those reported for the C^{sp2}=O and C^{sp2}–N moieties.[36] On the other hand, the bidentate coordination [C1–Rh–N8 85.21(8)°] of the ligand I^{Dipp}Amd causes a significant deviation of the NHC core from the ideal arrangement with respect to the Rh–C1 bond (NHC: pitch ϑ 4.0°; yaw ψ 12.1°).[37]

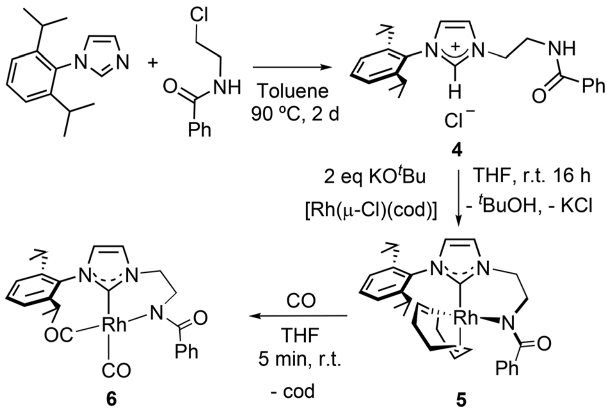

Scheme 2 Preparation of amidato-functionalized NHC rhodium derivatives **5** and **6**.

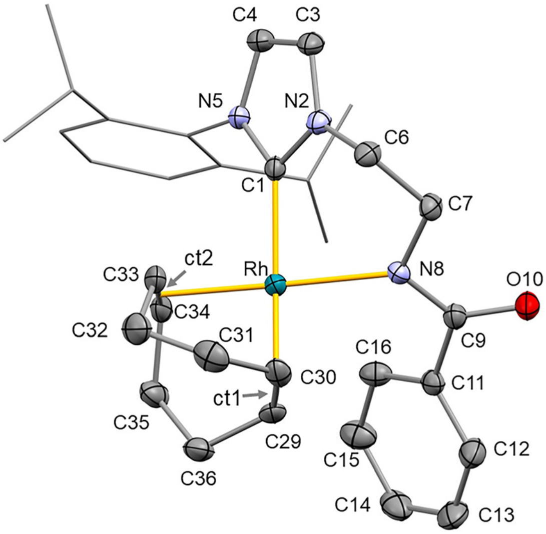

Fig. 4 ORTEP view of the crystal structure of Rh{κ^2*C*,*N*-(I^{Dipp}Amd)}(cod) (**5**). For clarity, hydrogen atoms are omitted and the 2,6-iPr$_2$C$_6$H$_3$ group is shown in a wireframe style. Thermal ellipsoids are at 50% probability. Selected bond lengths (Å) and angles (°) are: Rh–ct1 2.100(3), Rh–ct2 2.006(3), C1–Rh 2.044(2), N8–Rh 2.123(2), C9–N8 1.327(3), C9–O10 1.263(3), C29–C30 1.382(4), C33–C34 1.401(4), ct1–Rh–ct2 87.00(10), C1–Rh–N8 85.21(8), C9–N8–C7 111.9(2), C9–N8–Rh 130.27(16), C7–N8–Rh 117.78(15); ct1, centroid of C29 and C30; ct2, centroid of C33 and C34.

The NMR spectrum of **5** in CD$_2$Cl$_2$ at room temperature displays broad signals, showcasing the fluxional behaviour of the molecule, which is likely associated to the ring-flipping process of the six-membered metallacycle. However, well-defined resonances were observed in the ^{1}H NMR spectrum at 263 K. In contrast to **2** and **3**, an out-of-plane disposition of the NHC ring is observed for **5**. Thus, as a consequence of the lack of symmetry, the methylene protons of the linker are diastereotopic and display two doublets of doublets of doublets at δ 5.25 and 4.38 ppm for N$_{NHC}$CH$_2$ protons, and a multiplet at 3.52 ppm for the N$_{Amd}$CH$_2$ protons. Also, the four olefin cod protons and the two CH$_{Dipp}$ hydrogen atoms are inequivalent. The coordination of the carbene to the rhodium atom is supported by a doublet at δ 178.5 ppm (J_{C-Rh} = 53.7) in the ^{13}C{^{1}H}-APT NMR spectrum. The substitution of cod by two carbonyl ligands in **6** results in a steric relief that allows the NHC ring to adopt an in-plane disposition resulting in C_s symmetry. This is reflected in the chemical equivalence of the protons of both methylene linkers of the NHC-amidato ligand. Moreover, the ^{13}C{^{1}H}-APT spectrum shows two doublets at 186.9 (J_{C-Rh} = 63.0, CO$_{cis\text{-NHC}}$) and 184.9 ppm (J_{C-Rh} = 58.2, CO$_{trans\text{-NHC}}$) which confirms the presence of two carbonyl ligands in **6**.

Synthesis and characterization of NHC-carboxylato Rh(I) complexes

Complex Rh{κ^2*C*,*O*-(I^{Dipp}Carbx)}(cod) (**8**), featuring a carboxylato-functionalized NHC ligand, was prepared in a similar way to that described for **2** and **5** from the known 1-(2-carboxyethyl)-3-(2,6-diisopropylphenyl)-imidazol-3-ium chloride salt

(7)[38] and isolated as a yellow solid in 85% yield. The proposed structure shows a seven-membered metallacycle resulting from the bidentate κ^2*C*,*O* coordination of the ligand (Scheme 3). In fact, the difference between the asymmetric (1601 cm^{-1}) and symmetric (1375 cm^{-1}) carboxylato stretching bands in the infrared spectrum supports a κ^1*O*-carboxylato coordination.[39] An analogous chelate structure has been described for a Pd–NHC–carboxylato derivative.[40] Similar to **5**, complex **8** exhibits a fluxional process that is frozen at 213 K. However, the energy barrier for the inversion of the seven-membered NHC-carboxylato metallacycle of **8** is expected to be lower than that of the six-membered metalacycle of **5**, for which well-resolved signals are observed upon cooling to 263 K. At 213 K, the ^{1}H NMR spectrum of **8** displays two sets of signals for the diastereotopic methylene protons and the CH-isopropyl groups of the NHC wingtips. The ^{1}H–^{1}H NMR NOESY experiment at 213 K shows misleading cross-peaks due to a spin diffusion effect, therefore ^{1}H–^{1}H NMR ROESY experiment was recorded instead, confirming the proposed structure for **8** (see Fig. S30 in SI). Moreover, the carbene carbon atom is observed as a doublet at δ 178.4 ppm with a $J_{\text{C–Rh}}$ of 54.4 Hz in the ^{13}C{^{1}H}-APT spectrum.

Interestingly, the NHC-carboxylato complex **8** exhibits a distinct reactivity compared to the NHC-pyridonato (**2**) and NHC-amidato (**5**) analogues upon exposure to carbon monoxide. Thus, in addition to the expected square planar bis-carbonyl complex Rh{κ^2*C*,*O*-(I$^{\text{Dipp}}$Carbx)}(CO)$_2$ **9a**, a structural isomer **9b** was detected in a **9a** : **9b** 52 : 48 equilibrium ratio in solution at 233 K, confirmed by the exchange peaks observed in the EXSY NMR experiment (Fig. S36 in SI). Compound **9a** exhibits in the ^{13}C{^{1}H}-APT NMR spectrum the two expected low field doublets for the inequivalent carbonyl ligands at δ 186.8 and 186.7 ppm, with a $J_{\text{C–Rh}}$ of 56.0 and 58.2 Hz, respectively. However, the two CO ligands in **9b** are equivalent, showing a single resonance at 186.4 ppm ($J_{\text{C–Rh}}$ = 69.0 Hz) (Fig. 5). A plausible explanation for this observation is the description of **9b** as adopting a saw-horse or pseudo-tetrahedral structure.[41] Nonetheless, at this point an Y-shaped three coordinated zwiterionic species, bearing a dangling carboxylate, or a dinuclear A-frame structure could not be ruled out. A transoid disposition for two carbonyl ligands within Rh$^{\text{I}}$ derivatives is rare but not unprecedented.[42]

Reaction of the mixture of **9a** and **9b** with IPr {IPr = 1,3-bis-(2,6-diisopropylphenyl)-imidazolin-2-carbene} in THF gave the mixed-NHC complex Rh{κ^2*C*,*O*-(I$^{\text{Dipp}}$Carbx)}(CO)(IPr) (**10**), which was isolated as a white solid in 92% yield. The ^{1}H NMR spectrum revealed a single isomer displaying the characteristic signals of both IPr and I$^{\text{Dipp}}$Carbx carbene ligands, and a single carbonyl ligand. Thus, three doublets at δ 191.2 ($J_{\text{C–Rh}}$ = 79.5 Hz, CO), 189.5 ($J_{\text{C–Rh}}$ = 43.3 Hz, Rh–C$_{\text{IPr}}$), 185.7 ppm ($J_{\text{C–Rh}}$ = 43.1 Hz, Rh–C$_{\text{NHC–carbx}}$) and one singlet at 174.3 ppm for the κ^1*O*-carboxylato ligand appear in the low field region of the ^{13}C{^{1}H}-APT NMR spectrum of **10**. The spectroscopic data are consistent with a structure in which both NHC moieties adopt a *trans* arrangement to minimize steric repulsion (Scheme 4).[43]

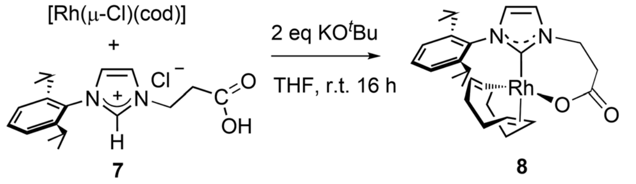

Scheme 3 Preparation of carboxylato-functionalized NHC rhodium derivative **8**.

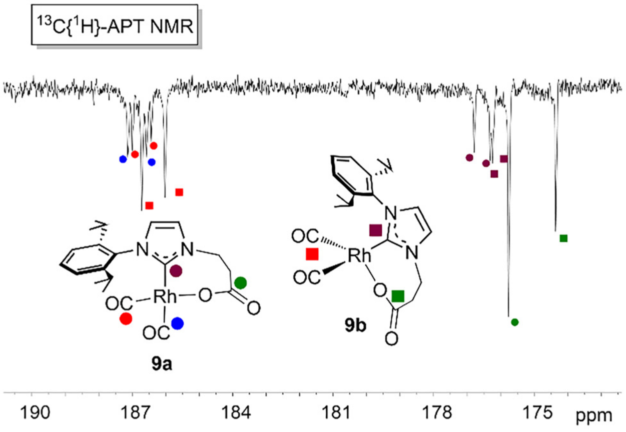

Fig. 5 Selected region of the ^{13}C{^{1}H}-APT NMR spectrum at 233 K of the equilibrium mixture of **9a**, **9b**.

Protonation of NHC–BHetA ligands

In order to assess the ability of the anionic functionalized NHC ligands in proton transfer processes, we investigated the protonation and deprotonation of the cod complexes **2**, **5** and **8**. Protonation was carried out by adding 1.5 equivalents of triflic acid to 0.5 mL of CD$_2$Cl$_2$ (**2** and **5**) or CDCl$_3$ (**8**) solutions of the BHetA complexes in an NMR tube at 223 K (Scheme 5). Formation of protonated species **11–13** was immediately observed by ^{1}H NMR measurements at 223 K. No high-shielded signal attributable to the putative Rh(III)–hydride

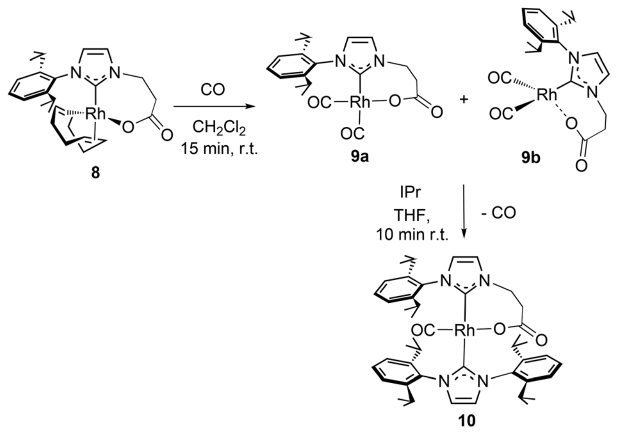

Scheme 4 Preparation of carboxylato-functionalized NHC rhodium carbonyl derivatives **9–10**.

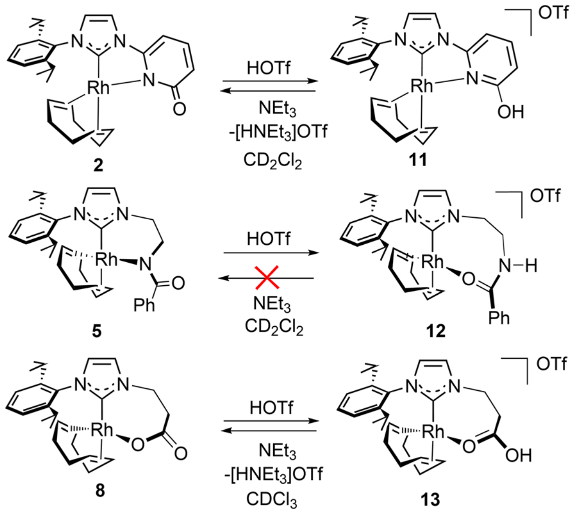

Scheme 5 Acid–base equilibrium for Rh–cod complexes **2**, **5** and **8**.

species, previously observed upon protonation of the IPr-chlorido analogue $[Rh(\mu\text{-}Cl)IPr(\eta^2\text{-}coe)]_2$,[44] was detected in the ^1H NMR spectra. It is noteworthy that the complexes remain stable in solution for over 24 hours upon warming the reaction mixture to room temperature, with no evidence of imidazolium salt formation.[17] Strong evidence for the cationic character of the complexes is provided by the detection of a single fluorine signal at δ −78.8 ppm in the ^{19}F NMR spectra. Protonation of the pyridonato complex **2** occurs at the oxygen atom, leading to the formation of a hydroxypyridine moiety to give $[Rh\{\kappa^2C,N\text{-}(I^{Dipp}OpyH)\}(cod)]OTf$ (**11**). In agreement with the proposed formation of the OH group, the broad signal at δ 11.46 ppm does not correlate with any nitrogen atom in the ^1H–^{15}N HMQC NMR spectrum. Moreover, the resonances corresponding to the protons of the heterocyclic ring (H_{10} and H_{12}) shifted downfield upon protonation. In contrast to that observed for **2**, protonation of the amidato derivative **5** takes place at the nitrogen atom resulting in the formation of the cationic complex $[Rh\{\kappa^2C,O\text{-}(I^{Dipp}AmdH)\}(cod)]OTf$ (**12**). The new N–H signal appears as a broad triplet at δ 9.13 ppm and correlates with a nitrogen atom at 114.0 ppm in the ^1H–^{15}N J^1-HMQC NMR spectrum. The observed nitrogen NMR chemical shift, falling in a similar range to that observed for the free ligand **4** (106.8 ppm), agrees with an uncoordinated nitrogen atom for **12**. In addition, the presence of a free triflate anion inferred by ^{19}F NMR suggests that the amide carbonyl group is likely coordinated given rise to an eight-membered metallacycle.[45] In the case of the protonation of the carboxylato complex **8**, the changes in the NMR signals were less pronounced than those observed for the pyridonato and amidato derivatives. Nevertheless, the observation of diastereotopic methylene protons supports the presence of a metallacycle motif in $[Rh\{\kappa^2C,O\text{-}(I^{Dipp}CarbxH)\}(cod)]OTf$ (**13**).

Next, the deprotonation of **11–13** was studied. Two equivalents of triethylamine were added to NMR tubes containing solutions of freshly formed **11–13** at room temperature. Within 10 minutes, the hydroxypyridine and carboxylic acid complexes were deprotonated, reverting to their respective parent complexes **2** and **8**, respectively (Fig. 6). In contrast, the amide complex **12** remained unchanged for several days at room temperature, and heating the sample at 60 °C led to the decomposition of the complex. Interestingly, it was observed that in $CDCl_3$ the amidato complex **5** transform into a new species $RhCl\{\kappa^2C,O\text{-}(I^{Dipp}AmdH)\}(cod)$ (**14**),[15c] after 3 days at room temperature under day light conditions, likely induced by trace amounts of hydrochloric acid generated from $CDCl_3$ over time (Scheme 6). In contrast, the pyridonato and carboxylato derivatives remain stable under $CDCl_3$ solutions for a week. The distinct behaviour of the amidato complex can be explained by its higher basicity. Therefore, the susceptibility of the amidato moiety to protonation, along with its resistance to deprotonation in the presence of a base such as triethylamine, may represent a limitation in catalytic processes involving proton transfer.

Catalytic reactions

Different mechanistic pathways can be invoked for alkyne dimerization, including oxidative addition, vinylidene, external nucleophilic attack, base mediated, or LAPS.[20,33] In addition, alkyne oligomerization or polymerization can be competitive

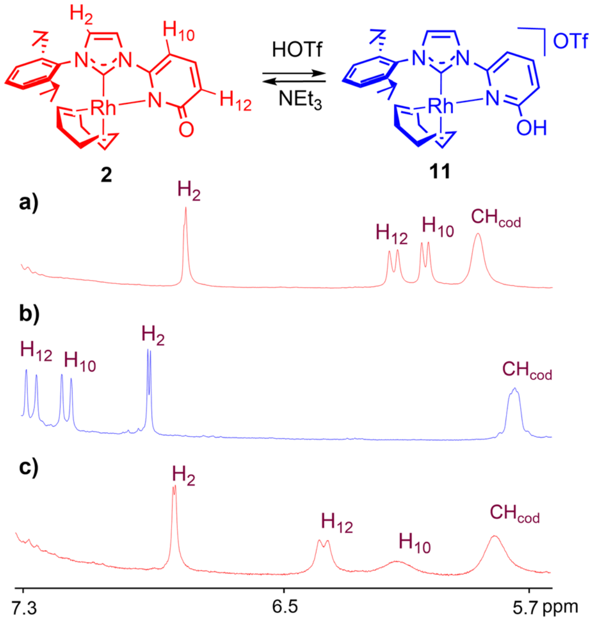

Fig. 6 (a) Selected region of the ^1H NMR spectrum of **2** in CD_2Cl_2. (b) treatment of **2** with HOTf to yield **11**. (c) **11** after addition of NEt_3.

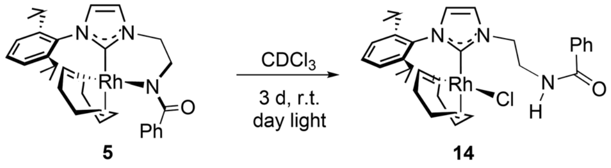

Scheme 6 Formation of Rh-chlorido complex **14**.

processes. In this context, we have recently disclosed that the presence of an internal base in Rh–NHC catalysts, such as a BHetA ligand, enhances the reactivity, but the catalytic outcome varies as a function of the ancillary ligand (Scheme 7). Thus, in the presence of a labile cyclooctene ligand the 1,3-*gem*-enynes are obtained *via* a LAPS process,[33] but in the case of a CO ligand a (2 + 2 + 1) cyclotrimerization results in the formation of fulvenes.[24] The effect of attaching a BHetA moiety at the wingtip of a NHC ligand has now been investigated.

The alkyne *tert*-butylacetylene was chosen as a benchmark substrate because of the versatile chemoselectivity previously observed in function of the catalyst employed. Catalytic reactions were performed in NMR tubes in C_6D_6 (0.5 mL) using a 5 mol% of catalyst loading at 90 °C for 72 h (Table 1). Conversion and selectivity were monitored by ^1H NMR spectroscopy. The cod derivatives with pyridonato (**2**) or amidato (**5**) ligands are less active than their CO counterparts **3** and **6**, showing high *gem*-selectivity of 80 and 95%, respectively (entries 1 and 3), whereas NHC-carboxylato complex **8** is inactive (entry 5). In contrast, the CO-pyridonato compound **3** is the most active of the series but with reverse regioselectivity towards the *E*-enyne. Furthermore, small amounts of fulvene (4%) were also detected (entry 2). The fulvene quantity slightly increases when using the amidato-CO catalyst **6**, but with a concomitant decrease in both activity and regioselectivity (entry 4). Carboxylato-CO catalyst **9** was unselective, whereas the bis-NHC compound **10** was completely inactive.

Table 1 Dimerization of *t*-butylacetylene catalyzed by different Rh(I) complexes with BHetA functionalized NHC ligands[a]

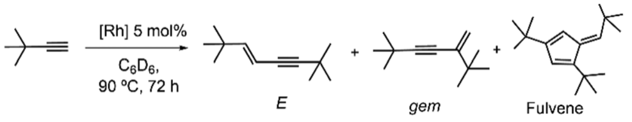

Entry	Catalyst	Conversion[b] (%)	Selectivity[b] (%) *E*/*gem*/fulvene
1	**2**	22	20/80/—
2	**3**	83	88/8/4
3	**5**	14	5/95/—
4	**6**	67	26/64/10
5	**8**	—	—/—/—
6	**9**	16	28/71/—
7	**10**	—	—/—/—

[a] Experiments were carried out in C_6D_6 (0.5 mL) at 90 °C using an alkyne/catalyst ratio of 100/5, [catalyst] = 20 mM. [b] Conversion and selectivity were determined by ^1H NMR.

The most active catalyst **3** was subsequently evaluated for other alkynes (Table 2). Selectivity to *E*-enynes was maintained for the substrates studied although with slightly lower values ranging from 58–72%. In the case of triisopropylsilyl and aromatic alkynes also the *Z*-enyne was also formed.

Catalytic results can be analysed on the basis of our previous mechanistic studies on untethered NHC–BHetA analogues (Scheme 7).[20,24,33] The predominant formation of the *gem*-enyne from cod derivatives suggests a proton-transfer mechanism *via* LAPS promoted by the BHetA-type pyridonato or amidato ligands (Scheme 6a), although alternative pathways including oxidative addition or base-mediated could not be excluded. However, the relatively low activity of these catalysts

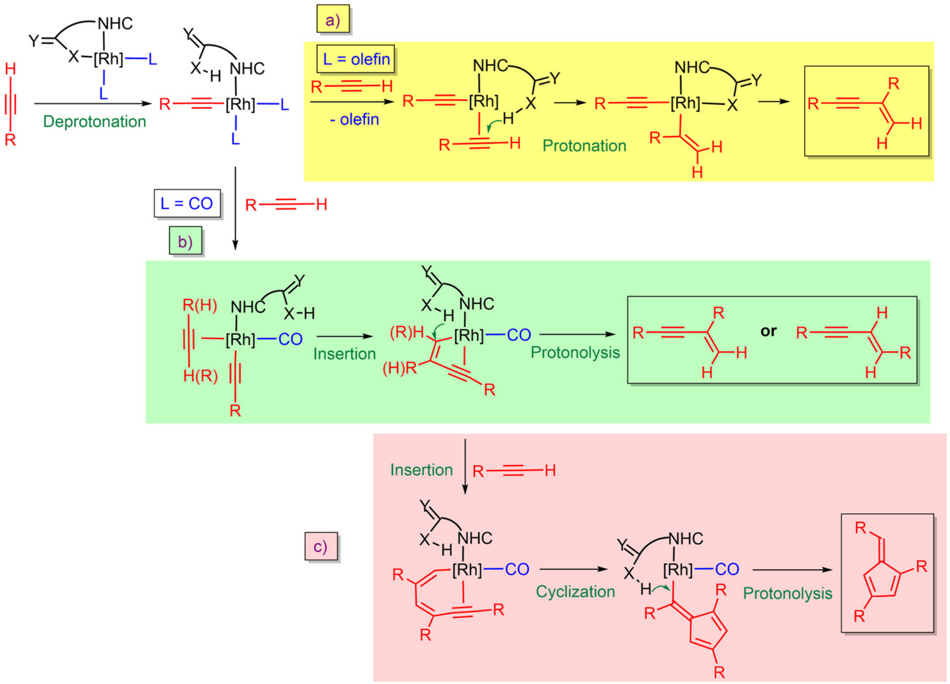

Scheme 7 Proposed mechanistic pathways for alkyne functionalization. (a) LAPS, (b) base-mediated, (c) fulvene formation *via* interrupted dimerization.

Table 2 Dimerization of different terminal alkynes catalyzed by **3** [a]

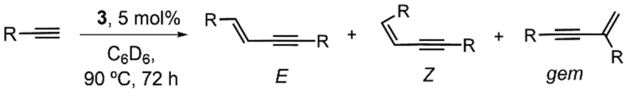

Entry	Alkyne	Conversion[a] (%)	Selectivity[b] (%), *E*/*Z*/*gem*
1	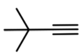	83	88/—/8
2	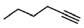	48	67/—/33
3	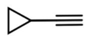	63	68/—/32
4	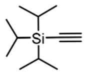	78	64/27/9
5	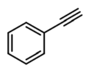	77	68/21/11
6	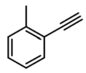	93	58/14/28
7	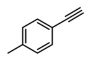	53	72/17/11
8	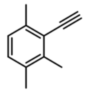	82	60/14/26

[a] Experiments were carried out in C_6D_6 (0.5 mL) at 90 °C using an alkyne/catalyst ratio of 100/5, [**3**] = 20 mM. [b] Conversion and selectivity were determined by ^{1}H NMR.

may be attributed to the strongly bound cod ligand, in contrast to the more labile monoolefin ligand present in untethered Rh (NHC)(BHetA)(coe) catalysts.[33] At this point, the low activity associated to the carboxylato ligand is unexplained but is consistent with previous observations for related Rh–NHC-carboxylato catalysts.[20] Conversely, the reversed selectivity towards *E*-enynes and trace formation of fulvenes observed for CO-bearing catalysts, suggests an insertion process as the regioselectivity-determining step (Scheme 7b and c).

Conclusion

A series of rhodium(I) complexes featuring anionic-tethered NHC-functionalized scaffolds, including pyridonato, amidato, and carboxylato functionalities, and bearing cod or CO as ancillary ligands, has been prepared and their application in alkyne homocoupling has been investigated. The chameleonic behavior of the pendant N-heterocyclic moiety is evidenced by its appearance as the hydroxypyridine tautomer in the salt, while it adopts a pyridonato form in the complexes. A coplanar arrangement of NHC and pyridonato rings within a five-membered metallacycle has been observed. In contrast, amidato-NHC derivatives feature a six-membered metallacycle which adopts a boat conformation. Moreover, NHC-carboxylato complexes display seven-membered metallacycle structures. The lability of one CO ligand in bis-CO NHC-carboxylato species enables the preparation of a mixed bis NHC complex. Protonation of the anionic ligand is reversible, except in the case of the NHC-amidato counterpart, for which the formation of an eight-membered metallacycle is proposed. Alkyne dimerization catalytic activity is observed for N-based anionic groups whereas their carboxylato counterparts are inactive. A proton transfer mechanism is proposed to account for the *gem*-selectivity observed with COD-based catalysts, whereas alkyne insertion constitutes the regioselectivity-determining step for CO-containing analogues. Further studies are currently underway in our laboratories to develop more efficient catalysts featuring anionic-tethered NHC motifs.

Experimental

General considerations

All reactions were carried out with rigorous exclusion of air and moisture using Schlenk-tube techniques and a dry box when necessary. Reagents were purchased from commercial suppliers and used as received except for alkynes which were dried over molecular sieves. Particularly, phenylacetylene was first dried over molecular sieves and then distilled and stored over anhydrous $CaCl_2$. Organic solvents were obtained oxygen- and water-free from a Solvent Purification System (Innovative Technologies). Deuterated solvents were dried and deoxygenated prior to use: C_6D_6 and toluene-d_8 with sodium, CD_2Cl_2 with calcium hydride, and $CDCl_3$ and CD_3CN with molecular sieves. The organometallic precursor $[Rh(\mu\text{-}Cl)(cod)]_2$ [46] and the imidazolium salts **1** [34] and **7**,[38] were prepared as previously described in the literature. NMR chemical shifts (expressed in parts per million) are referenced to residual solvent peaks (^{1}H and ^{13}C) or external $CFCl_3$ (^{19}F) and NH_3 (^{15}N). Coupling constants, *J*, are given in hertz (Hz). Spectral assignments were achieved by combination of ^{1}H, ^{13}C{^{1}H}-APT, ^{1}H–^{1}H COSY, and ^{1}H–^{13}C HSQC and HMBC experiments. The 2D ^{1}H–^{15}N HMQC long range experiments were recorded with a J_{N-H} = 8 or 4 Hz. Attenuated total reflection infrared spectra (ATR-IR) of solid samples were recorded on a PerkinElmer Spectrum 100 FT-IR spectrometer. C, H, and N analyses were carried out in a PerkinElmer 2400 CHNS/O analyzer. High-resolution electrospray ionization mass spectra (HRMS-ESI) were recorded using a Bruker MicroToF-Q equipped with an API-ESI source and a Q-ToF mass analyzer, which leads to a maximum error in the measurement of 5 ppm, using sodium formate as a reference.

Synthesis procedures and characterization data of Rh–NHC complexes

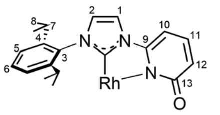

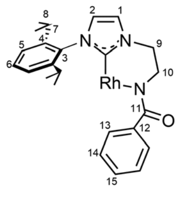

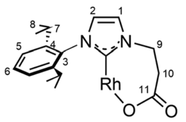

Preparation of Rh{κ^2*C*,*N*-(I^{Dipp}Opy)}(cod) (2). A mixture of **1** (300 mg, 0.75 mmol) and potassium *tert*-butoxide (250 mg, 2.23 mmol) in THF (20 mL) was stirred at 253 K for 10 min.

Then, a solution of $[Rh(\mu\text{-}Cl)(cod)]_2$ (182 mg, 0.37 mmol) in THF (10 mL) at 253 K was transferred to the reaction mixture. After stirring for 10 min at 253 K, the mixture was allowed to warm to room temperature and stirred for additional 30 min. The solvent was removed *in vacuo* and the residue dissolved in toluene (20 mL) and filtered through Celite. After concentration of the filtrate to *ca.* 1 mL, the addition of *n*-hexane (3 mL) produced the precipitation of an orange solid that was washed with *n*-hexane (3 × 5 mL) and dried *in vacuo*. Yield: 145 mg (37%). Anal. calcd for $C_{28}H_{34}N_3ORh\cdot1.5(CH_2Cl_2)$: C, 53.77; H, 5.66; N, 6.38. Found: C, 54.22; H, 6.03; N, 6.01. HRMS (ESI) *m*/*z* calcd for $C_{28}H_{35}N_3ORh$ $[M + H]^+$: 532.1835, found: 532.1832. ^1H NMR (500.1 MHz, $CDCl_3$, 298 K): δ 7.45 (t, J_{H-H} = 7.8, 1H, H_6), 7.40 (d, J_{H-H} = 1.8, 1H, H_1), 7.23 (d, J_{H-H} = 7.8, 2H, H_5), 7.20 (dd, J_{H-H} = 8.7, 7.8, 1H, H_{11}), 6.66 (d, J_{H-H} = 1.8, 1H, H_2), 6.34 (d, J_{H-H} = 8.7, 1H, H_{12}), 6.18 (m, 2H, $CH_{cod-\textit{trans}\text{-}NHC}$), 6.04 (d, J_{H-H} = 7.1, 1H, H_{10}), 3.50 (m, 2H, $CH_{cod-\textit{cis}\text{-}NHC}$), 2.72 (sept, J_{H-H} = 6.8, 2H, H_7), 2.2–1.7 (8H, $CH_{2\text{-}cod}$), 1.39 and 1.08 (both d, J_{H-H} = 6.8, 12H, H_8). $^{13}C\{^1H\}$-APT NMR (125.8 MHz, $CDCl_3$, 298 K): δ 174.7 (d, J_{C-Rh} = 56.6, $Rh-C_{NHC}$), 171.9 (C=O), 150.1 (C_9), 145.6 (C_4), 137.6 (C_{11}), 134.5 (C_3), 130.8 (C_6), 124.9 (C_2), 124.2 (C_5), 119.4 (C_{12}), 114.7 (C_1), 105.0 (d, J_{C-Rh} = 6.7, $CH_{cod-\textit{trans}\text{-}NHC}$), 89.8 ($C_{10}$), 70.8 (d, J_{C-Rh} = 12.4, $CH_{cod-\textit{cis}\text{-}NHC}$), 31.5 and 30.0 ($CH_{2\text{-}cod}$), 28.5 ($C_7$), 26.0 and 22.5 ($C_8$). $^1H-^{15}N$ HMQC (long range) NMR (40.5 MHz, $CDCl_3$, 298 K): δ 214.0 ($N_{NHC-Opy}$), 195.8 (N_{Opy}), 185.9 ($N_{NHC-Dipp}$).

Preparation of $Rh\{\kappa^2C,N\text{-}(I^{Dipp}Opy)\}(CO)_2$ (3). Carbon monoxide was bubbled through a yellow solution of **2** (100 mg, 0.19 mmol) in dichloromethane (20 mL) for 15 min at room temperature. After removing the solvent *in vacuo*, *n*-hexane was added to induce the precipitation of a yellow solid, which was washed with *n*-hexane (3 × 5 mL) and dried *in vacuo*. Yield: 70 mg (78%). Anal. calcd for $C_{22}H_{22}N_3O_3Rh$: C, 55.13; H, 4.63; N, 8.67. Found: C, 55.37; H, 4.13; N, 8.45. IR (cm^{-1}, ATR): 2075 $\nu(CO)_{sym}$, 2005 $\nu(CO)_{asym}$. ^1H NMR (400.1 MHz, CD_2Cl_2, 243K): δ 7.54 (d, J_{H-H} = 2.0, 1H, H_1), 7.52 (t, J_{H-H} = 7.6, 1H, H_6), 7.33 (d, J_{H-H} = 7.8, 2H, H_5), 7.26 (dd, J_{H-H} = 8.7, 6.8, 1H, H_{11}), 7.05 (d, J_{H-H} = 2.0, 1H, H_2), 6.36 (d, J_{H-H} = 8.7, 1H, H_{12}), 6.16 (d, J_{H-H} = 6.8, 1H, H_{10}), 2.56 (sept, J_{H-H} = 6.8, 2H, H_7), 1.29 and 1.19 (both d, J_{H-H} = 6.8, 12H, H_8). $^{13}C\{^1H\}$-APT NMR (100.1 MHz, CD_2Cl_2, 243K): δ 188.1 (d, J_{C-Rh} = 57.0, $CO_{\textit{trans}\text{-}NHC}$), 187.3 (d, J_{C-Rh} = 68.1, $CO_{\textit{cis}\text{-}NHC}$), 181.8 (d, J_{C-Rh} = 48.7, $Rh-C_{NHC}$), 167.6 (C=O), 150.4 (C_9), 146.5 (C_4), 139.2 (C_{11}), 135.2 (C_3), 131.6 (C_6), 125.0 (C_5), 124.7 (C_2), 117.2 (C_{12}), 116.5 (C_1), 90.3 (C_{10}), 28.9 (C_7), 24.7 and 23.9 (C_8).

Preparation of $[I^{Dipp}AmdH_2]Cl$ (4). A mixture of 1-(2,6-diisopropylphenyl)imidazole (456 mg, 2.00 mmol) and *N*-(2-chloroethyl)benzamide (367 mg, 2.00 mmol) in toluene (5 mL) was stirred at 363 K for 2 days. Then, the solution was allowed to cool to room temperature, and diethyl ether (20 mL) was added. The precipitate formed was filtered, washed with a diethyl ether–toluene mixture (9/1, 3 × 10 mL) and dried *in vacuo*. Yield: 610 mg (74%). Anal. calcd for $C_{24}H_{30}N_3OCl.0.5(H_2O)$: C, 68.47; H, 7.42; N, 9.98. Found: C, 68.58; H, 7.66; N, 9.92. ^1H NMR (300 MHz, $CDCl_3$, 298 K): δ 10.17 (s, 1H, NCHN), 9.32 (t, J_{H-H} = 4.4, 1H, NH), 8.18 (d, J_{H-H} = 6.5, 2H, H_{13}), 7.81 (br, 1H, H_1), 7.5–7.4 (m, 4H, $H_{6,14,15}$), 7.22 (d, J_{H-H} = 7.9, 2H, H_5), 7.26 (m, 1H, H_2), 5.19 (br, 2H, H_9), 4.18 (br, 2H, H_{10}), 2.08 (sept, J_{H-H} = 6.8, H7), 0.97 and 0.91 (both d, J_{H-H} = 6.8, 12H, H_8). $^{13}C\{^1H\}$-APT NMR (75 MHz, $CDCl_3$, 298 K): δ 168.1 (C=O), 145.5 (C_4), 138.9 (NCHN), 132.8 (C_{12}), 132.0 (C_6), 131.8 (C_{15}), 130.1 (C_3), 128.6 (C_{14}), 128.0 (C_{13}), 124.7 (C_5), 124.3 (C_2), 123.4 (C_1), 49.2 (C_9), 39.2 (C_{10}), 28.7 (C_7), 24.4 and 23.9 (C_8). $^1H-^{15}N$ HMQC (long range) NMR (40.5 MHz, $CDCl_3$, 298 K): δ 183.0 ($N_{NHC-Dipp}$), 179.8 ($N_{NHC-Amd}$), 106.4 (NH_{Amd}).

Preparation of $Rh\{\kappa^2C,N\text{-}(I^{Dipp}Amd)\}(cod)$ (5). This compound was prepared as described for **2** starting from **4** (334 mg, 0.81 mmol), potassium *tert*-butoxide (182 mg, 1.62 mmol) and $[Rh(\mu\text{-}Cl)(cod)]_2$ (200, 0.41 mmol) with a reaction time of 16 h at room temperature. Yellow solid, yield: 290 mg (61%). Anal. calcd for $C_{32}H_{40}N_3ORh$: C, 65.63; H, 6.88; N, 7.18. Found: C, 65.87; H, 7.14; N, 7.33. ^1H NMR (400.1 MHz, CD_2Cl_2, 263 K): δ 8.36 (d, J_{H-H} = 6.5, 2H, H_{13}), 7.50 (t, J_{H-H} = 7.7, 1H, H_6), 7.4–7.2 (5H, $H_{5,14,15}$), 7.15 (d, J_{H-H} = 1.7, 1H, H_1), 6.76 (d, J_{H-H} = 1.7, 1H, H_2), 5.25 (ddd, J_{H-H} = 13.1, 12.1, 5.1, 1H, H_9), 4.72 (m, 1H, $CH_{cod-\textit{trans}\text{-}NHC}$), 4.38 (ddd, J_{H-H} = 13.1, 2.9, 2.3, 1H, H_9), 3.52 (m, 2H, H_{10}), 3.45 (m, 1H, $CH_{cod-\textit{cis}\text{-}NHC}$), 3.22 (m, 1H, $CH_{cod-\textit{cis}\text{-}NHC}$), 2.97 and 2.20 (both sept, J_{H-H} = 6.7, 2H, H_7), 2.44 (m, 1H, $CH_{cod-\textit{trans}\text{-}NHC}$), 2.4–1.1 (m, 8H, $CH_{2\text{-}cod}$), 1.42, 1.16, 1.08, and 0.88 (all d, J_{H-H} = 6.7, 6H, H_8). $^{13}C\{^1H\}$-APT NMR (100.1 MHz, CD_2Cl_2, 263 K): δ 178.5 (d, J_{C-Rh} = 53.7, $Rh-C_{NHC}$), 173.7 (C=O), 146.5 and 146.3 (C_4), 142.5 (C_{12}), 135.6 (C_3), 130.4 (C_6), 129.1 (C_{15}), 128.1 (C_{13}), 127.3 (C_{14}), 123.9 (C_2), 123.8 and 123.7 (C_5), 120.4 (C_1), 97.2 (d, J_{C-Rh} = 8.8, $CH_{cod-\textit{trans}\text{-}NHC}$), 88.5 (d, J_{C-Rh} = 7.3, $CH_{cod-\textit{trans}\text{-}NHC}$), 72.4 (d, J_{C-Rh} = 11.9, $CH_{cod-\textit{cis}\text{-}NHC}$), 70.0 (d, J_{C-Rh} = 12.3, $CH_{cod-\textit{cis}\text{-}NHC}$), 52.1 ($C_9$), 46.6 ($C_{10}$), 34.9, 32.4, 29.2, and 26.1 ($CH_{2\text{-}cod}$), 28.7 and 28.2 (C_7), 26.8, 26.3, 22.6, and 22.2 (all s, C_8). $^1H-^{15}N$ HMQC (long range) NMR (40.5 MHz, $CDCl_3$, 263 K): δ 188.1 ($N_{NHC-Dipp}$), 187.7 ($N_{NHC-Amd}$).

Preparation of $Rh\{\kappa^2C,N(I^{Dipp}Amd)\}(CO)_2$ (6). Carbon monoxide was bubbled through a yellow solution of **5** (100 mg, 0.17 mmol) in THF (20 mL) for 5 min at room temperature. After removing the solvent *in vacuo*, *n*-hexane was added to induce the precipitation of an orange solid, which was washed with *n*-hexane (3 × 5 mL) and dried *in vacuo*. Yield: 60 mg (63%). IR (cm^{-1}, ATR): 2065 $\nu(CO)_{sym}$, 1994 $\nu(CO)_{asym}$. Accurate elemental analysis could not be obtained. HRMS (ESI) *m*/*z* calcd for $C_{25}H_{29}N_3O_2Rh$ $[M + H - CO]^+$: 506.1315, found: 506.1337. ^1H NMR (400.1 MHz, toluene-d_8, 298 K): δ 8.10 (m, 2H, H_{13}), 7.24 (t, J_{H-H} = 7.2, 1H, H_6), 7.3–7.0 (5H, $H_{5,14,15}$), 6.86 (br, 1H, H_1), 6.48 (br, 1H, H_2), 3.98 (m, 2H, H_9), 3.84 (m, 2H, H_{10}), 2.61 (sept, J_{H-H} = 6.8, 2H, H_7), 1.30 and 0.96 (both d, J_{H-H} = 6.8, 12H, H_8). $^{13}C\{^1H\}$-APT NMR (100.1 MHz, toluene-d_8, 298 K): δ 186.9 (d, J_{C-Rh} = 63.0, $CO_{\textit{cis}\text{-}NHC}$), 184.9 (d, J_{C-Rh} = 58.2, $CO_{\textit{trans}\text{-}NHC}$), 176.8 (C=O), 174.0 (d, J_{C-Rh} = 49.1, $Rh-C_{NHC}$), 146.5 (C_4), 145.0 (C_{12}), 137.5 (C_3), 131.0 (C_6), 129.0 (C_{15}), 128.4 (C_{13}), 127.4 (C_{14}), 124.4 (C_5), 124.0 (C_2), 122.8 (C_1), 51.9 (C_{10}), 44.3 (C_9), 28.9 (C_7), 25.5 and 23.0 (C_8).

Preparation of $Rh\{\kappa^2C,O\text{-}(I^{Dipp}Carbx)\}(cod)$ (8). This compound was prepared as described **5** starting from **7** (270 mg, 0.81 mmol) potassium *tert*-butoxide (182 mg, 1.62 mmol) and [Rh(μ-Cl)(cod)]$_2$ (200, 0.41 mmol). Yellow solid, yield: 348 mg (85%). IR (cm^{-1}, ATR): 1601 ν(OCO)$_{asym}$, 1375 ν(OCO)$_{sym}$. Accurate elemental analysis could not be obtained. HRMS (ESI) *m*/*z* calcd for $C_{26}H_{36}N_2O_2Rh$ [M + H]$^+$: 511.1832, found: 511.1826. ^{1}H NMR (400.1 MHz, CD$_2$Cl$_2$, 213 K): δ 7.45 (t, J_{H-H} = 7.5, 1H, H$_6$), 7.35 and 7.14 (both d, J_{H-H} = 7.5, 2H, H$_5$), 7.06 (br, 1H, H$_1$), 6.77 (br, 1H, H$_2$), 5.82 (t, J_{H-H} = 12.9, 1H, H$_9$), 4.63 and 4.53 (both m, 2H, CH$_{\text{cod–}trans\text{-NHC}}$), 4.15 (d, J_{H-H} = 12.9, 1H, H$_9$), 3.39 (m, 2H, CH$_{\text{cod–}cis\text{-NHC}}$), 2.7 (m, 2H, H$_{10}$), 2.47 and 2.05 (both sept, J_{H-H} = 6.5, 2H, H$_7$), 2.3–1.7 (8H, CH$_{2\text{-cod}}$), 1.80, 1.04, 0.98, and 0.97 (all d, J_{H-H} = 6.5, 12H, H$_8$). ^{13}C{^{1}H}-APT NMR (100.1 MHz, CDCl$_3$, 213 K): δ 178.4 (J_{C-Rh} = 54.4, Rh–C$_{NHC}$), 175.6 (OCO), 146.9 and 144.8 (C$_4$), 134.2 (C$_3$), 129.7 (C$_6$), 124.3 and 123.2 (C$_5$), 124.2 (C$_2$), 119.9 (C$_1$), 98.5 and 98.2 (both br, CH$_{\text{cod–}trans\text{-NHC}}$), 65.6 and 63.5 (bot d, J_{C-Rh} = 12.4, CH$_{\text{cod–}cis\text{-NHC}}$), 47.9 (C$_9$), 38.2 (C$_{10}$), 34.3, 31.8, 28.1, and 27.4 (CH$_{2\text{-cod}}$), 28.4 and 27.8 (C$_7$), 25.8, 25.3, 24.8, and 22.9 (C$_8$).

Preparation of Rh{κ^2*C*,*O*-(I$^{\text{Dipp}}$Carbx)}(CO)$_2$, (9a,b). This compound was prepared as described for **3** starting from **8** (150 mg, 0.30 mmol). Pale yellow solid, yield: 92 mg (69%). IR (cm^{-1}, ATR): 2070 ν(CO)$_{sym}$, 1990 ν(CO)$_{asym}$, 1613 ν(OCO)$_{asym}$, 1383 ν(OCO)$_{sym}$. NMR data evidenced the presence of two isomers **9a** and **9b** in a 52 : 48 ratio. HRMS (ESI) *m*/*z* calcd for $C_{20}H_{24}N_2O_4Rh$ [M + H]$^+$: 459.0791, found: 459.0786.

9a: ^{1}H NMR (400.1 MHz, CD$_2$Cl$_2$, 233 K): δ 7.64 (d, J_{H-H} = 2.0, 1H, H$_1$), 7.49 (t, J_{H-H} = 7.7, 1H, H$_6$), 7.29 (d, J_{H-H} = 7.7, 1H, H$_5$), 6.96 (d, J_{H-H} = 2.0, 1H, H$_2$), 4.64 (t, J_{H-H} = 5.1, 2H, H$_9$), 2.70 (t, J_{H-H} = 5.1, 2H, H$_{10}$), 2.44 (sept, J_{H-H} = 6.5, 2H, H$_7$), 1.20 and 1.01 (both d, J_{H-H} = 6.5, 12H, H$_8$). ^{13}C{^{1}H}-APT NMR (100.1 MHz, CD$_2$Cl$_2$, 233 K): δ 186.8 (d, J_{C-Rh} = 56.0, CO$_{trans\text{-NHC}}$), 186.7 (d, J_{C-Rh} = 58.2, CO$_{cis\text{-NHC}}$), 176.0 (d, J_{C-Rh} = 47.8, Rh–C$_{NHC}$), 175.8 (OCO), 146.1 (C$_4$), 134.9 (C$_3$), 130.2 (CH$_6$), 124.7 (C$_2$), 124.1 (CH$_5$), 122.6 (C$_1$), 48.5 (C$_9$), 37.4 (C$_{10}$), 28.4 (C$_7$), 26.4 and 22.5 (C$_8$).

9b: ^{1}H NMR (400 MHz, CD$_2$Cl$_2$, 233 K): δ 7.49 (t, J_{H-H} = 7.7, 1H, H$_6$), 7.28 (d, J_{H-H} = 7.7, 1H, H$_5$), 7.21 (d, J_{H-H} = 1.7, 1H, H$_1$), 7.04 (d, J_{H-H} = 1.7, 1H, H$_2$), 4.49 (t, J_{H-H} = 9.0, 2H, H$_9$), 2.84 (t, J_{H-H} = 9.0, 2H, H$_{10}$), 2.45 (sept, J_{H-H} = 6.5, 2H, H$_7$), 1.14 and 1.01 (both d, J_{H-H} = 6.5, 12H, H$_8$). ^{13}C{^{1}H}-APT NMR (100 MHz, CDCl$_3$, 233 K): δ 186.4 (d, J_{C-Rh} = 69.0, 2C, CO), 176.6 (d, J_{C-Rh} = 47.9, Rh–C$_{NHC}$), 174.4 (s, OCO), 146.0 (s, C$_4$), 134.9 (s, C$_3$), 130.2 (s, CH$_6$), 124.9 (C$_2$), 124.1 (s, CH$_5$), 121.2 (C$_1$), 48.6 (s, C$_9$), 38.0 (s, C$_{10}$), 28.4 (C$_7$), 26.3 and 22.7 (C$_8$).

Preparation of Rh{κ^2*C*,*O*-(I$^{\text{Dipp}}$Carbx)}(CO)(IPr) (10). A THF (10 mL) solution of **9a** and **9b** (55 mg, 0.12 mmol) and IPr (47 mg, 0.12 mmol) was stirred at room temperature for 10 min. Then, the solvent was removed *in vacuo* and the addition of *n*-hexane (3 mL) produced the precipitation of a white solid that was washed with *n*-hexane (3 × 5 mL) and dried *in vacuo*. Yield: 90 mg (92%). IR (cm^{-1}): 1948 ν(CO), 1627 ν(OCO)$_{asym}$, 1367 ν(OCO)$_{sym}$. Accurate elemental analysis could not be obtained. HRMS (ESI) *m*/*z* calcd for $C_{46}H_{60}N_4O_3Rh$ [M + H]$^+$: 819.3720, found: 819.3715. ^{1}H NMR (300 MHz, C$_6$D$_6$, 298 K): δ 7.33 (m, 2H, H$_{p\text{-IPr}}$), 7.23–7.19 (m, 4H, H$_{m\text{-IPr}}$), 7.20 (m, 1H, H$_6$), 7.03 (d, J_{H-H} = 7.7, 2H, H$_5$), 6.60 (s, 2H, =CHN$_{IPr}$), 6.27 (d, J_{H-H} = 1.6, 1H, H$_1$), 5.97 (d, J_{H-H} = 1.6, 1H, H$_2$), 3.71 (m, 2H, H$_9$), 3.09 (sept, J_{H-H} = 6.7, 4H, C$\underline{\text{H}}$Me$_{IPr}$), 2.51 (sept, J_{H-H} = 6.7, 2H, H$_{7a}$), 2.41 (m, 2H, H$_{10}$), 1.43 and 1.06 (both d, J_{H-H} = 6.7, 24H, Me$_{IPr}$), 1.09 and 0.94 (both d, J_{H-H} = 6.8, 12H, H$_8$). ^{13}C{^{1}H}-APT NMR (75 MHz, C$_6$D$_6$, 298 K): δ 191. 2 (d, J_{C-Rh} = 79.5, CO), 189.5 (d, J_{C-Rh} = 43.3, Rh–C$_{IPr}$), 185.7 (d, J_{C-Rh} = 43.1, Rh–C$_{NHC}$), 174.3 (OCO), 147.1 (C$_{q\text{-IPr}}$), 146.8 (C$_4$), 137.1 (C$_q$N$_{IPr}$), 136.4 (C$_3$), 129.8 (C$_{p\text{-IPr}}$), 129.4 (C$_6$), 124.1 (=CHN$_{IPr}$), 124.0 (C$_{m\text{-IPr}}$), 123.7 (C$_5$), 123.5 (C$_2$), 119.7 (C$_1$), 47.9 (C$_9$), 42.2 (C$_{10}$), 28.8 ($\underline{\text{C}}$HMe$_{IPr}$), 28.7 (C$_7$), 26.4 and 23.1 (Me$_{IPr}$), 25.9 and 23.9 (C$_8$).

***In situ* formation of [Rh{κ^2*C*,*N*-(I$^{\text{Dipp}}$OpyH)}(cod)]OTf (11).** A solution of **2** (21 mg, 0.04 mmol) in CD$_2$Cl$_2$ at 243 K (0.5 mL, NMR tube) was treated with trifluoromethanesulfonic acid (5 μL, 0.06 mmol). NMR spectra were recorded immediately at low temperature. ^{1}H NMR (400.1 MHz, CD$_2$Cl$_2$, 243K): δ 11.46 (br, OH), 7.92 (t, J_{H-H} = 8.0, 1H, H$_{11}$), 7.73 (br, 1H, H$_1$), 7.54 (t, J_{H-H} = 7.8, 1H, H$_6$), 7.31 (d, J_{H-H} = 7.8, 2H, H$_5$), 7.14 (m, 2H, H$_{10,12}$), 6.90 (br, 1H, H$_2$), 5.83 (m, 2H, CH$_{\text{cod–}trans\text{-NHC}}$), 3.72 (m, 2H, CH$_{\text{cod–}cis\text{-NHC}}$), 2.63 (sept, 2H, J_{H-H} = 6.8, H$_7$), 2.3–1.7 (m, 8H, CH$_{2\text{cod}}$), 1.38 and 1.08 (both d, J_{H-H} = 6.8, 12H, H$_8$). ^{13}C{^{1}H}-APT NMR (100.1 MHz, CD$_2$Cl$_2$, 243K): δ 173.7 (d, J_{C-Rh} = 55.3, Rh–C$_{NHC}$), 166.3 (C=O), 149.9 (C$_9$), 145.0 (C$_4$), 144.3 (C$_{11}$), 133.4 (C$_3$), 131.2 (C$_6$), 126.4 (C$_2$), 124.4 (C$_5$), 120.8 (q, J_{C-F} = 320.1, CF$_3$), 115.9 (C$_1$), 111.2 (C$_{12}$), 101.7 (C$_{10}$), 104.4 (d, J_{C-Rh} = 6.5, CH$_{\text{cod–}trans\text{-NHC}}$), 72.9 (d, J_{C-Rh} = 13.3, CH$_{\text{cod–}cis\text{-NHC}}$), 31.4 and 29.4 (both s, CH$_{2\text{-cod}}$), 28.5 (C$_7$), 25.8 and 22.2 (both s, C$_8$). ^{1}H–^{15}N HMQC (long range) NMR (40.5 MHz, CD$_2$Cl$_2$, 243K): δ 209.6 (N$_{NHC-OPy}$), 198.9 (N$_{OPy}$), 189.8 (N$_{NHC-Dipp}$). ^{19}F NMR (282.3 MHz, CD$_2$Cl$_2$, 243 K): δ −78.8.

***In situ* formation of Rh[{κ^2*C*,*O*-(I$^{\text{Dipp}}$AmdH)}(cod)]OTf (12).** This compound was prepared as described for **11** starting from **5** (24 mg, 0.04 mmol) and trifluoromethanesulfonic acid (5 μL, 0.06 mmol). ^{1}H NMR (400.1 MHz, CD$_2$Cl$_2$, 243K): δ 9.13 (t, J_{H-H} = 6.9, 1H, N–H), 7.79 (m, 2H, H$_{13}$), 7.6–7.5 (m, 2H, H$_{6,15}$), 7.48 (m, 2H, H$_{14}$), 7.36 (m, 1H, H$_9$), 7.31 (m, 2H, H$_5$), 7.27 (d, J_{H-H} = 1.9, 1H, H$_1$), 6.87 (d, J_{H-H} = 1.9, 1H, H$_2$), 4.80 and 4.69 (both m, 2H, CH$_{\text{cod–}trans\text{-NHC}}$), 4.19 (m, 1H, H$_9$), 3.81 and 3.05 (both m, 2H, CH$_{\text{cod–}cis\text{-NHC}}$), 2.78 (sept, J_{H-H} = 6.8, 1H, H$_7$), 1.90 (m, 1H, H$_7$), 2.51 and 1.95 (m, 2H, H$_{10}$), 2.5–1.3 (m, 8H, CH$_{2\text{cod}}$), 1.58, 1.31, 1.12, and 0.63 (all d, J_{H-H} = 6.8, 12H, H$_8$). ^{13}C{^{1}H}-APT NMR (75 MHz, CD$_2$Cl$_2$, 298 K): δ 178.6 (d, J_{C-Rh} = 51.6, Rh–C$_{NHC}$), 173.1 (C=O), 146.2 (C$_4$), 145.7 (C$_{12}$), 135.7 (C$_3$), 132.6 (C$_6$), 130.2 (C$_{15}$), 128.5 (C$_{14}$), 127.3 (C$_{13}$), 124.7 (C$_2$), 124.6 (C$_1$), 124.2 and 123.8 (C$_5$), 120.1 (q, J_{C-F} = 318.9, CF$_3$), 99.4 and 95.1 (both d, J_{C-Rh} = 7.5, CH$_{\text{cod–}trans\text{-NHC}}$), 67.6 and 67.2 (both d, J_{C-Rh} = 15.2, CH$_{\text{cod–}cis\text{-NHC}}$), 51.3 (C$_9$), 39.1 (C$_{10}$), 34.2, 31.5, 30.4, and 27.4 (all s, CH$_{2\text{cod}}$), 28.4 and 28.1 (C$_7$), 25.9, 24.9, 22.7, and 22.5 (all s, C$_8$). ^{1}H–^{15}N HMQC (long range) NMR (40.5 MHz, CD$_2$Cl$_2$, 263 K): δ 192.8 (N$_{NHC-Dipp}$), 187.9 (N$_{NHC-Amd}$), 114.3 (NH$_{amd}$). ^{19}F NMR (282.3 MHz, CD$_2$Cl$_2$, 243 K): δ −78.9.

***In situ* formation of Rh[{κ^2*C*,*O*-(I$^{\text{Dipp}}$CarbxH)}(cod)]OTf (13).** This compound was prepared as described for **11** starting from **8** (45 mg, 0.08 mmol) and trifluoromethanesulfonic acid

(10 μL, 0.12 mmol). ^{1}H NMR (400 MHz, $CDCl_3$, 243 K): δ 7.51 (t, J_{H-H} = 7.5, 1H, H_6), 7.42 and 7.22 (both d, J_{H-H} = 7.5, 2H, H_5), 7.19 (m, 1H, H_1), 6.85 (m, 2H, H_2), 5.29 and 4.83 (both m, 1H, H_9), 4.79 (m, 2H, $CH_{cod-\textit{trans}-NHC}$), 3.49 (m, 1H, H_{10}), 3.47 (m, 1H, $CH_{cod-\textit{cis}-NHC}$), 3.28 (m, 1H, H_{10}), 2.86 (m, 1H, $CH_{cod-\textit{cis}-NHC}$), 2.5–1.4 (m, 8H, CH_{2cod}), 1.98 (sept, J_{H-H} = 6.8, 1H, H_7), 1.88 (m, 1H, H_7), 1.55 and 0.98 (both d, J_{H-H} = 6.8, 6H, H_8), 1.13 (m, 6H, H_8). $^{13}C\{^1H\}$-APT NMR (100.1 MHz, $CDCl_3$, 298 K): δ 181.2 (d, J_{C-Rh} = 51.3, Rh–C_{NHC}), 177.5 (C=O), 147.5 and 145.1 (C_4), 135.4 (C_3), 129.9 (C_6), 124.6 (C_2), 124.5 and 123.3 (C_5), 121.5 (C_1), 97.9 and 97.0 (both d, J_{C-Rh} = 5.4, $CH_{cod-\textit{trans}-NHC}$), 68.7 and 68.1 (both d, J_{C-Rh} = 14.0, $CH_{cod-\textit{cis}-NHC}$), 46.6 ($C_9$), 35.8 ($C_{10}$), 34.5, 30.9, 29.6, and 27.6 (all s, CH_{2cod}), 28.4 and 28.3 (C_7), 26.7, 26.2, 23.8, and 22.9 (all s, C_8). ^{19}F NMR (282.3 MHz, $CDCl_3$, 243 K): δ −78.7.

***In situ* formation of RhCl{κ^2*C*,*O*-(I^{Dipp}AmdH)}(cod) (14).** A solution of **5** (24 mg, 0.04 mmol) in $CDCl_3$ (0.5 mL, NMR tube) was kept in day light conditions at room temperature for 3 days. ^{1}H NMR (400.1 MHz, $CDCl_3$, 298 K): δ 8.37 (d, J_{H-H} = 7.7, 1H, N–H), 8.00 (d, J_{H-H} = 7.2, 2H, H_{13}), 7.49 (t, J_{H-H} = 7.7, 1H, H_6), 7.4–7.3 (m, 4H, $H_{5,14,15}$), 7.23 (dd, J_{H-H} = 7.7, 1.3, 1H, $H_{5'}$), 7.19 (d, J_{H-H} = 2.0, 1H, H_1), 6.82 (d, J_{H-H} = 2.0, 1H, H_2), 6.07 and 4.42 (both m, 2H, H_9), 4.8–4.7 (m, 2H, $CH_{cod-\textit{trans}-NHC}$), 4.65 and 3.73 (both m, 2H, H_{10}), 3.58 and 2.94 (both m, 2H, $CH_{cod-\textit{cis}-NHC}$), 3.26 and 2.10 (both sept, J_{H-H} = 6.8, 2H, H_7), 2.5–1.3 (m, 8H, CH_{2cod}), 1.43, 1.17, 1.13, and 0.58 (all d, J_{H-H} = 6.8, 12H, H_8). $^{13}C\{^1H\}$-APT NMR (100.1 MHz, $CDCl_3$, 298 K): δ 182.9 (d, J_{Rh-C} = 51.6, Rh–C_{NHC}), 168.1 (C=O), 147.7 (C_4), 145.0 (C_{12}), 135.4 (C_3), 131.2 (C_6), 129.8 (C_{15}), 128.2 (C_{14}), 127.6 (C_{13}), 125.4 (C_2), 124.3 and 123.3 (C_5), 118.9 (C_1), 98.3 (d, J_{Rh-C} = 7.1, $CH_{cod-\textit{trans}-NHC}$), 97.0 (d, J_{Rh-C} = 7.3, $CH_{cod-\textit{trans}-NHC}$), 69.1 (d, J_{Rh-C} = 14.7, $CH_{cod-\textit{cis}-NHC}$), 67.2 (d, J_{Rh-C} = 14.7, $CH_{cod-\textit{cis}-NHC}$), 48.5 ($C_9$), 37.8 ($C_{10}$), 34.9, 30.5, 29.8, and 27.3 (all s, CH_{2cod}), 28.4 and 28.3 (C_7), 26.7, 25.4, 23.2, and 22.6 (all s, C_8).

Catalytic alkyne dimerization reactions. Alkyne dimerization catalytic reactions were carried out in NMR tubes under argon atmosphere. In a typical procedure, an NMR tube was charged with the catalyst (5 mol%, 0.01 mmol), C_6D_6 (0.5 mL) and alkyne (0.20 mmol). The solution was kept in a thermostatic bath at 363 K and monitored by ^{1}H NMR spectroscopy. The reaction products were unambiguously characterized on the basis NMR literature data.[24,29b,31a,b,47] Conversion and selectivities were determined by ^{1}H NMR spectroscopy.

Crystal structure determination. X-ray diffraction data were collected on Bruker Smart Apex (2), Apex Duo CCD (5) and D8 Venture (1) diffractometers with graphite-monochromated Mo-Kα radiation (λ = 0.71073 Å) using ω rotations. Intensities were integrated and corrected for absorption effects with SAINT–PLUS[48] and SADABS[49] programs, both included in APEX3 package. The structures were solved by the Patterson method with SHELXS-97[50] and refined by full matrix least-squares on F^2 with SHELXL-2014,[51] under WinGX.[52] After the structural refinement, the residual electron density in 2 and 5 was treated using the program Squeeze (Platon).[53] Pitch and yaw angles have been calculated according to the literature.[37]

Crystal data and structure refinement for 1. $C_{21}H_{25}BrCl_3N_3O$, 521.70 g mol^{-1}, 100(2) K, monoclinic, $P2_1/n$, a = 11.9779(6) Å, b = 14.1815(7) Å, c = 14.4172(9) Å, β = 100.042(2)°, V = 2411.5(2) Å^3, Z = 4, D_{calc} = 1.437 g cm^{-3}, μ = 2.054 mm^{-1}, F(000) = 1064, 0.150 × 0.120 × 0.080 mm^3, $\theta_{min}/\theta_{max}$ 2.030/27.101°, index ranges $-15 \le h \le 15$, $-18 \le k \le 18$, $-18 \le l \le 16$, reflections collected/independent 64 512/5318 [R(int) = 0.0486], T_{max}/T_{min} 0.7458/0.6765, data/restraints/parameters 5318/30/294, GoF(F^2) = 1.061, R_1 = 0.0481 [$I > 2\sigma(I)$], wR_2 = 0.1240 (all data), largest diff. peak/hole 0.953/−1.017 e Å^{-3}. CCDC deposit number 2464206.

Crystal data and structure refinement for 2. $C_{28}H_{34}N_3ORh\cdot1.5(CH_2Cl_2)$, 658.88 g mol^{-1}, 100(2) K, monoclinic, $P2_1/n$, a = 9.8550(15) Å, b = 10.5806(16) Å, c = 28.689(4) Å, β = 96.195(2)°, V = 2974.0(8) Å^3, Z = 4, D_{calc} = 1.472 g cm^{-3}, μ = 0.871 mm^{-1}, F(000) = 1356, 0.250 × 0.200 × 0.170 mm^3, $\theta_{min}/\theta_{max}$ 2.053/28.361°, index ranges $-13 \le h \le 13$, $-14 \le k \le 14$, $-37 \le l \le 38$, reflections collected/independent 34 483/7311 [R(int) = 0.0449], T_{max}/T_{min} 0.8132/0.7353, data/restraints/parameters 7311/0/303, GoF(F^2) = 1.125, R_1 = 0.0469 [$I > 2\sigma(I)$], wR_2 = 0.1061 (all data), largest diff. peak/hole 1.066/−1.297 e Å^{-3}. CCDC deposit number 2464205.

Crystal data and structure refinement for 5. $C_{32}H_{40}N_3ORh\cdot0.5(C_6H_{14})$, 628.66 g mol^{-1}, 120(2) K, monoclinic, $C2/c$, a = 33.795(4) Å, b = 11.1748(12) Å, c = 18.4247(19) Å, β = 119.0060(10)°, V = 6085.3(11) Å^3, Z = 8, D_{calc} = 1.372 g cm^{-3}, μ = 0.593 mm^{-1}, F(000) = 2648, 0.250 × 0.240 × 0.070 mm^3, $\theta_{min}/\theta_{max}$ 1.378/26.368°, index ranges $-42 \le h \le 42$, $-13 \le k \le 13$, $-23 \le l \le 23$, reflections collected/independent 52 609/6223 [R(int) = 0.0614], T_{max}/T_{min} 0.9010/0.7685, data/restraints/parameters 6223/0/338, GoF(F^2) = 1.038, R_1 = 0.0302 [$I > 2\sigma(I)$], wR_2 = 0.0753 (all data), largest diff. peak/hole 0.785/−0.720 e Å^{-3}. CCDC deposit number 2464207.

Conflicts of interest

There are no conflicts to declare.

Data availability

Data supporting this article is including in SI. Supplementary information is available. See DOI: https://doi.org/10.1039/d5dt01516b.

CCDC 2464205–2464207 (**2**, **1**, and **5**) contain the supplementary crystallographic data for this paper.[54a–c]

Acknowledgements

Financial support from the Spanish Ministerio de Ciencia, Innovación y Universidades MICIU/AEI/10.13039/501100011033, under the Projects PID2019-103965GB-I00 and PID2022-137208NB-I00, and the Departamento de Ciencia, Universidad y Sociedad del Conocimiento del Gobierno de Aragón (group E42_23R) is gratefully acknowledged. MOK thankfully acknowledge the University of Zaragoza for a contract under the program "Researchers Affected by Natural Disasters". The use of the Servicio General de Apoyo a la Investigación-SAI of the University of Zaragoza, and the scientific-technical services of the ISQCH/CEQMA (CSIC) is gratefully acknowledged.

References

1 (*a*) A. J. Arduengo III and L. I. Iconaru, *Dalton Trans.*, 2009, 6903–6914; (*b*) P. Belotti, M. Koy, M. N. Hopkinson and F. Glorius, *Nat. Rev. Chem.*, 2021, **5**, 711–725.

2 (*a*) L. Oehninger, R. Rubbiani and I. Ott, *Dalton Trans.*, 2013, **42**, 3269–3284; (*b*) Y.-F. Zhang, Y.-K. Yin, H. Zhang and Y.-F. Han, *Coord. Chem. Rev.*, 2024, **514**, 215941.

3 (*a*) C. A. Smith, M. R. Narouz, P. A. Lummis, I. Singh, A. Nazemi, C.-H. Li and C. M. Crudden, *Chem. Rev.*, 2019, **119**, 4986–5056; (*b*) H. Amouri, *Chem. Rev.*, 2023, **123**, 230–270.

4 (*a*) W. A. Herrmann, *Angew. Chem., Int. Ed.*, 2002, **41**, 1290–1309; (*b*) D. Enders, O. Niemeier and A. Henseler, *Chem. Rev.*, 2007, **107**, 5606–5655; (*c*) Q. Zhao, G. Meng, S. P. Nolan and M. Szostak, *Chem. Rev.*, 2020, **120**, 1981–2048; (*d*) Q. Liang and D. Song, *Chem. Soc. Rev.*, 2020, **49**, 1209–1232; (*e*) J. Thongpaen, R. Manguin and O. Baslé, *Angew. Chem., Int. Ed.*, 2020, **59**, 10242–10251.

5 L. Benhamou, E. Chardon, G. Lavigne, S. Bellemin-Laponnaz and V. César, *Chem. Rev.*, 2011, **111**, 2705–2733.

6 (*a*) H. Grützmacher, *Angew. Chem., Int. Ed.*, 2008, **47**, 1814–1818; (*b*) D. B. Grotjahn, *Dalton Trans.*, 2008, 6497–6508; (*c*) S. Kuwata and T. Ikariya, *Chem. Commun.*, 2014, **50**, 14290–14300; (*d*) J. R. Khusnutdinova and D. Milstein, *Angew. Chem., Int. Ed.*, 2015, **54**, 12236–12273; (*e*) B. Ramasamy and P. Ghosh, *Eur. J. Inorg. Chem.*, 2016, 1448–1465; (*f*) T. Higashi, S. Kusumoto and K. Nozaki, *Chem. Rev.*, 2019, **119**, 10393–10402.

7 (*a*) S. Hameury, P. de Fremont and P. Braunstein, *Chem. Soc. Rev.*, 2017, **46**, 632–733; (*b*) W. Stroek, N. A. V. Rowlinson, L. A. Hudson and M. Albrecht, *Inorg. Chem.*, 2024, **63**, 17134–17140.

8 (*a*) D. Pugh and A. A. Danopoulos, *Coord. Chem. Rev.*, 2007, **251**, 610–641; (*b*) E. M. Richards, L. Casarrubios, J. M. D'Oyley, H. S. Rzepa, A. J. P. White, K. Goldberg, F. W. Goldberg, J. A. Bull and S. Diéz-González, *Adv. Synth. Catal.*, 2025, **367**, e202400909.

9 (*a*) S. Gaillard and J.-L. Renaud, *Dalton Trans.*, 2013, **42**, 7255–7270; (*b*) S. Bhattacharya, B. Atwi, K. Kundu, W. Frey and M. R. Buchmeiser, *Organometallics*, 2025, **44**, 315–324.

10 (*a*) C. Fliedel and P. Braunstein, *J. Organomet. Chem.*, 2014, **751**, 286–300; (*b*) M. Hruzd, S. L. Kleynemeyer, C. Michon, S. Bastin, E. Pollet, V. Ritleng and J.-B. Sortais, *Chem. Commun.*, 2025, **61**, 2969–2972.

11 (*a*) G. Tan, S. Enthaler, S. Inoue, B. Blom and M. Driess, *Angew. Chem., Int. Ed.*, 2015, **54**, 2214–2218; (*b*) T. Komuro, K. Hayasaka, K. Takahashi, N. Ishiwata, K. Yamauchi, H. Tobita and H. Hashimoto, *Dalton Trans.*, 2024, **53**, 4041–4047.

12 (*a*) A. Zanardi, E. Peris and J. A. Mata, *New J. Chem.*, 2008, **32**, 120–126; (*b*) Q. Liang, K. M. Osten and D. Song, *Angew. Chem., Int. Ed.*, 2017, **56**, 6317–6320; (*c*) B. Sánchez-Page, J. Munarriz, M. V. Jiménez, J. J. Pérez-Torrente, J. Blasco, G. Subias, V. Passarelli and P. Álvarez, *ACS Catal.*, 2020, **10**, 13334–13351; (*d*) M. O. Karatas, B. Alıcı, V. Passarelli, I. Ozdemir, J. J. Pérez-Torrente and R. Castarlenas, *Dalton Trans.*, 2021, **50**, 11206–11215.

13 (*a*) S. T. Liddle, I. S. Edworthy and P. L. Arnold, *Chem. Soc. Rev.*, 2007, **36**, 1732–1744; (*b*) S. Bellemin-Laponnaz and S. Dagorne, *Chem. Rev.*, 2014, **114**, 8747–8774; (*c*) E. Peris, *Chem. Rev.*, 2018, **118**, 9988–10031.

14 (*a*) K. Fujita, R. Tamura, Y. Tanaka, M. Yoshida, M. Onoda and R. Yamaguchi, *ACS Catal.*, 2017, **7**, 7226–7230; (*b*) S. Siek, D. B. Burks, D. L. Gerlach, G. Liang, J. M. Tesh, C. R. Thompson, F. Qu, J. E. Shankwitz, R. M. Vasquez, N. Chambers, G. J. Szulczewski, D. B. Grotjahn, C. E. Webster and E. T. Papish, *Organometallics*, 2017, **36**, 1091–1106; (*c*) M. Huang, Y. Li, J. Liu, X.-B. Lan, Y. Liu, C. Zhao and Z. Ke, *Green Chem.*, 2019, **21**, 219–224; (*d*) P. Pandey, P. Daw, N. U. D. Reshi, K. R. Ehmann, M. Hölscher, W. Leitner and J. K. Bera, *Organometallics*, 2020, **39**, 3849–3863; (*e*) A. A. Kadam, M. Afandiyeva, W. Brennessel and C. R. Kennedy, *Organometallics*, 2024, **43**, 2574–2580; (*f*) H. A. G. Mayerstein and D. Song, *ACS Catal.*, 2024, **14**, 17489–17502.

15 (*a*) C.-Y. Liao, K.-T. Chan, J.-Y. Zeng, C.-H. Hu, C.-Y. Tu and H. M. Lee, *Organometallics*, 2007, **26**, 1692–1702; (*b*) J. Berding, T. F. van Dijkman, M. Lutz, A. L. Spek and E. Bouwman, *Dalton Trans.*, 2009, 6948–6955; (*c*) S. Warsink, J. A. Venter and A. Roodt, *J. Organomet. Chem.*, 2015, **775**, 195–201; (*d*) Z. Huang, S. Wang, X. Zhu, Q. Yuan, Y. Wei, S. Zhou and X. Mu, *Inorg. Chem.*, 2018, **57**, 15069–15078; (*e*) J. Cao, G. Xiong, Z. Luo, Q. Huang, W. Zhou, I. Dragutan, V. Dragutan, Y. Sun and F. Ding, *Inorg. Chim. Acta*, 2024, **568**, 122076.

16 (*a*) C. Gandolfi, M. Heckenroth, A. Neels, G. Laourenczy and M. Albrecht, *Organometallics*, 2009, **28**, 5112–5121; (*b*) J. Thongpaen, T. E. Schmid, L. Toupet, V. Dorcet, M. Mauduit and O. Baslé, *Chem. Commun.*, 2018, **54**, 8202–8205; (*c*) Y. Hu and S. Guo, *Appl. Organomet. Chem.*, 2019, **33**, e4703; (*d*) R. Manguin, M. Galiana-Cameo, T. Kittikool, C. Barthes, J. Thongpaen, E. Bancal, S. Mallet-Ladeira, S. Yotphan, R. Castarlenas, M. Mauduit, J.-B. Sortais and O. Baslé, *Chem. Commun.*, 2023, **59**, 4193–4196; (*e*) J. Sanz-Garrido, R. Andrés, C. González-Arellano and J. C. Flores, *Adv. Synth. Catal.*, 2025, **367**, e202401289.

17 (*a*) D. P. Allen, C. M. Crudden, L. A. Calhoun and R. Wang, *J. Organomet. Chem.*, 2004, **689**, 3203–3209; (*b*) L. Palacios, A. Di Giuseppe, A. Opalinska, R. Castarlenas, J. J. Pérez-Torrente, F. J. Lahoz and L. A. Oro, *Organometallics*, 2013, **32**, 2768–2774; (*c*) V. M. Chernyshev, E. A. Denisova, D. B. Eremin and V. P. Ananikov, *Chem. Sci.*, 2020, **11**, 6957–6977.

18 (*a*) R. Puerta-Oteo, M. V. Jiménez, F. J. Lahoz, F. J. Modrego, V. Passarelli and J. J. Pérez-Torrente, *Inorg. Chem.*, 2018, **57**, 5526–5543; (*b*) J. Sanz-Garrido, A. Martin, C. González-Arellano and J. C. Flores, *Dalton Trans.*, 2024, **53**, 1460–1468.

19 (*a*) B. M. Trost and J. T. Masters, *Chem. Soc. Rev.*, 2016, **45**, 2212–2238; (*b*) Q. Liang, K. Hayashi and D. Song, *ACS Catal.*, 2020, **10**, 4895–4905; (*c*) S. M. Weber and G. Hilt, *Front. Chem.*, 2021, **9**, 635826.

20 M. Galiana-Cameo, M. Borraz, Y. Zelenkova, V. Passarelli, F. J. Lahoz, J. J. Pérez-Torrente, L. A. Oro, A. Di Giuseppe and R. Castarlenas, *Chem. – Eur. J.*, 2020, **26**, 9598–9608.

21 A. Roglans, A. Pla-Quintana and M. Solà, *Chem. Rev.*, 2021, **121**, 1894–1979.

22 M. Angoy, M. V. Jiménez, P. García-Orduña, L. A. Oro, E. Vispe and J. J. Pérez-Torrente, *Organometallics*, 2019, **38**, 1991–2006.

23 L. Leroyer, M. Maraval and R. Chauvin, *Chem. Rev.*, 2012, **112**, 1310–1343.

24 B. Español-Sánchez, J. Moradell, M. Galiana-Cameo, E. Barrenas, J. J. Pérez-Torrente, V. Passarelli and R. Castarlenas, *Angew. Chem., Int. Ed.*, 2025, **64**, e202507424.

25 Y. Shibata, K. Noguchi and K. Tanaka, *Org. Lett.*, 2010, **12**, 5596–5599.

26 V. Claus, M. Schukin, S. Harrer, M. Rudolph, F. Rominger, A. M. Asiri, J. Xie and S. K. Hashmi, *Angew. Chem., Int. Ed.*, 2018, **57**, 12966–12970.

27 C. M. Storey, A. Kalpokas, M. R. Gyton, T. Krämer and A. B. Chaplin, *Chem. Sci.*, 2020, **11**, 2051–2057.

28 (*a*) M. Rubina and V. Gevorgyan, *J. Am. Chem. Soc.*, 2001, **123**, 11107–11108; (*b*) S. Ventre, E. Derat, M. Amatore, C. Aubert and M. Petit, *Adv. Synth. Catal.*, 2013, **355**, 2584–2590; (*c*) P. Żak, M. Bołt, J. Lorkowski, M. Kubicki and C. Pietraszuk, *ChemCatChem*, 2017, **9**, 3627–3631; (*d*) X. Zhuang, J.-Y. Chen, Z. Yang, M. Jia, C. Wu, R.-Z. Liao, C.-H. Tung and W. Wang, *Organometallics*, 2019, **38**, 3752–3759; (*e*) Y. Ueda, H. Tsurugi and K. Mashima, *Angew. Chem., Int. Ed.*, 2020, **59**, 1552–1556.

29 (*a*) M. Nishiura, Z. Hou, Y. Wakatsuki, T. Yamaki and T. Miyamoto, *J. Am. Chem. Soc.*, 2003, **125**, 1184–1185; (*b*) R. H. Platel and L. L. Schafer, *Chem. Commun.*, 2012, **48**, 10609–10611; (*c*) O. Rivada-Wheelaghan, S. Chakraborty, L. J. W. Shimon, Y. Ben-David and D. Milstein, *Angew. Chem., Int. Ed.*, 2016, **55**, 6942–6945; (*d*) N. Gorgas, L. G. Alves, B. Stöger, A. M. Martins, L. F. Veiros and K. Kirchner, *J. Am. Chem. Soc.*, 2017, **139**, 8130–8133; (*e*) N. Gorgas, B. Stöger, L. F. Veiros and K. Kirchner, *ACS Catal.*, 2018, **8**, 7973–7982; (*f*) J. E. Stevens, J. D. Miller, M. C. Fitzsimmons, C. E. Moore and C. M. Thomas, *Chem. Commun.*, 2024, **60**, 5169–5172.

30 (*a*) T. Chen, C. Guo, M. Goto and L.-B. Han, *Chem. Commun.*, 2013, **49**, 7498–7500; (*b*) G. Kleinhans, G. Guisado-Barrios, D. C. Liles, G. Bertrand and D. I. Bezuidenhout, *Chem. Commun.*, 2016, **52**, 3504–3507; (*c*) Q. Liang, K. Sheng, A. Salmon, V. Y. Zhou and D. Song, *ACS Catal.*, 2019, **9**, 810–818; (*d*) J.-F. Chen and C. Li, *ACS Catal.*, 2020, **10**, 3881–3889.

31 (*a*) L. Rubio-Pérez, R. Azpíroz, A. Di Giuseppe, V. Polo, R. Castarlenas, J. J. Pérez-Torrente and L. A. Oro, *Chem. – Eur. J.*, 2013, **19**, 15304–15314; (*b*) O. V. Zatolochnaya, E. G. Gordeev, C. Jahier, V. P. Ananikov and V. Gevorgyan, *Chem. – Eur. J.*, 2014, **20**, 9578–9588; (*c*) C. M. Storey, M. R. Gyton, R. E. Andrew and A. B. Chaplin, *Chem. – Eur. J.*, 2020, **26**, 14715–14723; (*d*) C. Pfeffer, N. Wannenmacher, W. Frey and R. Peters, *ACS Catal.*, 2021, **11**, 5496–5505; (*e*) Y. Sun, J. Zhang, Y. Zeng, L. Meng and X. Li, *J. Org. Chem.*, 2024, **89**, 605–616.

32 (*a*) H. Zhang and X. Bao, *RSC Adv.*, 2015, **5**, 84636–84642; (*b*) H. Chen, Z. Dang, X. Sha, Y. Wang, Z. Zhang, Y. Luo and Y. Lan, *ACS Catal.*, 2024, **14**, 16469–16478; (*c*) X. Wu and L. Zhang, *Org. Lett.*, 2024, **26**, 5736–5740.

33 (*a*) M. Galiana-Cameo, A. Urriolabeitia, E. Barrenas, V. Passarelli, J. J. Pérez-Torrente, A. Di Giuseppe, V. Polo and R. Castarlenas, *ACS Catal.*, 2021, **11**, 7553–7567; (*b*) B. Español-Sánchez, M. Galiana-Cameo, A. Urriolabeitia, V. Polo, V. Passarelli, J. J. Pérez-Torrente and R. Castarlenas, *Organometallics*, 2024, **43**, 2951–2962.

34 (*a*) A. Srinivasan, J. Campos, N. Giraud, M. Robert and O. Rivada-Wheelaghan, *Dalton Trans.*, 2020, **49**, 16623–16626; (*b*) M. Afandiyeva, A. A. Kadam, X. Wu, W. W. Brennessel and C. R. Kennedy, *Organometallics*, 2022, **41**, 3014–3023.

35 M. Breugst and H. Mayr, *J. Am. Chem. Soc.*, 2010, **132**, 15380–15389.

36 F. H. Allen, O. Kennard, D. G. Watson, L. Brammer, A. G. Orpen and R. Taylor, *J. Chem. Soc., Perkin Trans. 2*, 1987, S1–S19.

37 R. Azpíroz, L. Rubio-Pérez, A. Di Giuseppe, V. Passarelli, F. J. Lahoz, R. Castarlenas, J. J. Pérez-Torrente and L. A. Oro, *ACS Catal.*, 2014, **4**, 4244–4253.

38 C. Lohre, T. Dröge, C. Wang and F. Glorius, *Chem. – Eur. J.*, 2011, **17**, 6052–6055.

39 G. B. Deacon and R. J. Phillis, *Coord. Chem. Rev.*, 1980, **33**, 227–250.

40 N. E. Nigglia and O. Baudoin, *Helv. Chim. Acta*, 2021, **104**, e2100015.

41 D. Ostendorf, C. Landis and H. Grützmacher, *Angew. Chem., Int. Ed.*, 2006, **45**, 5169–5173.

42 See for example: (*a*) L. H. Pignolet, D. H. Doughty, S. C. Nowicki, M. P. Anderson and A. L. Casalnuovo, *J. Organomet. Chem.*, 1980, **202**, 211–223; (*b*) M. Montag, I. Efremenko, R. Cohen, G. Leitus, L. J. W. Shimon, Y. Diskin-Posner, Y. Ben-David, J. M. L. Martin and D. Milstein, *Chem. – Eur. J.*, 2008, **14**, 8183–8194; (*c*) R. E. Andrew, D. W. Ferdani, C. A. Ohlin and A. B. Chaplin, *Organometallics*, 2015, **34**, 913–917.

43 See: R. Azpíroz, M. O. Karataş, V. Passarelli, I. Özdemir, J. J. Pérez-Torrente and R. Castarlenas, *Molecules*, 2022, **27**, 7002, and references therein.

44 A. Di Giuseppe, R. Castarlenas, J. J. Pérez-Torrente, F. J. Lahoz and L. A. Oro, *Chem. – Eur. J.*, 2014, **20**, 8391–8403.

45 G. Storch, L. Deberle, J.-M. Menke, F. Rominger and O. Trapp, *Chirality*, 2016, **28**, 744–748.

46 J. Chatt and L. M. Venanzi, *J. Chem. Soc.*, 1957, 4735–4741.

47 A. Coniglio, M. Bassetti, S. E. García-Garrido and J. Gimeno, *Adv. Synth. Catal.*, 2012, **354**, 148–158.

48 *SAINT+: Area-Detector Integration Software, version 6.01*, Bruker AXS, Madison, WI, 2001.

49 G. M. Sheldrick, *SADABS program*, University of Göttingen, Göttingen, Germany, 1999.

50 G. M. Sheldrick, *SHELXS 97*, University of Göttingen, Göttingen, Germany, 1997.

51 G. M. Sheldrick, *Acta Crystallogr., Sect. C: Struct. Chem.*, 2015, **71**, 3–8.

52 L. J. Farrugia, *J. Appl. Crystallogr.*, 2012, **45**, 849–854.

53 A. L. Spek, *Acta Crystallogr., Sect. C: Struct. Chem.*, 2015, **71**, 9–18.

54 (*a*) M. O. Karataş, D. R. Hinojosa, V. Passarelli, L. A. Oro, J. J. Pérez-Torrente and R. Castarlenas, CCDC 2464205: Experimental Crystal Structure Determination, 2025, DOI: 10.5517/ccdc.csd.cc2nq6h3; (*b*) M. O. Karataş, D. R. Hinojosa, V. Passarelli, L. A. Oro, J. J. Pérez-Torrente and R. Castarlenas, CCDC 2464206: Experimental Crystal Structure Determination, 2025, DOI: 10.5517/ccdc.csd.cc2nq6j4; (*c*) M. O. Karataş, D. R. Hinojosa, V. Passarelli, L. A. Oro, J. J. Pérez-Torrente and R. Castarlenas, CCDC 2464207: Experimental Crystal Structure Determination, 2025, DOI: 10.5517/ccdc.csd.cc2nq6k5.